

interval measurements are needed to evaluate sudden, quick, and short-lasting BP changes comparable with continuous intra-arterial monitoring (54). On the other hand, another previous study compared the different measurement intervals of ambulatory BP monitoring and showed that a minimum sampling frequency of two readings per hour (i.e., a 30-min interval) is required to obtain an accurate assessment of short-term BP variability (55). Therefore, we believe that the method of one measurement for every 30 min in the present study can ensure a good assessment of ambulatory short-term BP variability (53).

In conclusion, the results of the present study showed that the intensified multifactorial medical therapy, including ARB and statin, improved ambulatory mean BP and short-term BP variability concomitant with the reduction of albuminuria without a decrease in eGFR in hypertensive patients with type 2 diabetic nephropathy. Particularly, the results of multivariate regression analysis showed a significant negative association between eGFR and nighttime systolic BP variability, in addition to that between eGFR and nighttime diastolic BP during the intensified multitherapy in the present study. Also, a recent subanalysis of ASCOT-BPLA study suggested that the better inhibitory effects of calcium channel blockers on ambulatory BP variability than b blockers account for the superiority of calcium channel blockers over b blockers in the suppression of cardiovascular events, irrespective of no significant difference in mean BP levels (34). Accumulated evidence already indicated that it is critically important to achieve the target BP goal to efficiently inhibit organ damages including diabetic nephropathy. As a next step, more and better evidence on the intensified multifactorial medical therapy-mediated beneficial effects on renal function and ambulatory BP profile including short-term BP variability could help to lead to a more precise understanding of the pathogenesis, and hence potential treatment, of diabetic nephropathy and its cardiovascular complications (56–58).

## ACKNOWLEDGMENTS

This work was supported in part by grants from the Japanese Ministry of Education, Science, Sports, and Culture, by Health and Labor Sciences Research grant; and by grants from the Yokohama Foundation for Advancement of Medical Science, Salt Science Research Foundation (No. 1033), Mitsubishi Pharma Research Foundation, and the Strategic Research Project of Yokohama City University.

**Declaration of interest:** The authors report no conflicts of interest. The authors alone are responsible for the content and writing of the paper.

## REFERENCES

- [1] Adler AI, Stevens RJ, Manley SE, Bilous RW, Cull CA, Holman RR. Development and progression of nephropathy in type 2 diabetes: the United Kingdom Prospective Diabetes Study (UKPDS 64). *Kidney Int* 2003;63:225–232.
- [2] Turner RC, Millns H, Neil HA, Stratton IM, Manley SE, Matthews DR, Holman RR. Risk factors for coronary artery disease in non-insulin dependent diabetes mellitus: United Kingdom Prospective Diabetes Study (UKPDS: 23). *BMJ* 1998;316:823–828.
- [3] Adler AI, Stratton IM, Neil HA, Yudkin JS, Matthews DR, Cull CA, Wright AD, Turner RC, Holman RR. Association of systolic blood pressure with macrovascular and microvascular complications of type 2 diabetes (UKPDS 36): prospective observational study. *BMJ* 2000;321:412–419.
- [4] Valmadrid CT, Klein R, Moss SE, Klein BE. The risk of cardiovascular disease mortality associated with microalbuminuria and gross proteinuria in persons with older-onset diabetes mellitus. *Arch Intern Med* 2000;160:1093–1100.
- [5] Gerstein HC, Mann JF, Yi Q, Zinman B, Dinneen SF, Hoogwerf B, Halle JP, Young J, Rashkow A, Joyce C, Nawaz S, Yusuf S. Albuminuria and risk of cardiovascular events, death, and heart failure in diabetic and nondiabetic individuals. *JAMA* 2001;286:421–426.
- [6] Ninomiya T, Perkovic V, de Galan BE, Zoungas S, Pillai A, Jardine M, Patel A, Cass A, Neal B, Poulter N, Mogensen CE, Cooper M, Marre M, Williams B, Hamet P, Mancia G, Woodward M, Macmahon S, Chalmers J. Albuminuria and kidney function independently predict cardiovascular and renal outcomes in diabetes. *J Am Soc Nephrol* 2009;20:1813–1821.
- [7] Drury PL, Ting R, Zannino D, Ehnholm C, Flack J, Whiting M, Fassett R, Ansquer JC, Dixon P, Davis TM, Pardy C, Colman P, Keech A. Estimated glomerular filtration rate and albuminuria are independent predictors of cardiovascular events and death in type 2 diabetes mellitus: the Fenofibrate Intervention and Event Lowering in Diabetes (FIELD) study. *Diabetologia* 2011; 54:32–43.
- [8] Gaede P, Vedel P, Larsen N, Jensen GV, Parving HH, Pedersen O. Multifactorial intervention and cardiovascular disease in patients with type 2 diabetes. *N Engl J Med* 2003;348:383–393.
- [9] Gaede P, Lund-Andersen H, Parving HH, Pedersen O. Effect of a multifactorial intervention on mortality in type 2 diabetes. *N Engl J Med* 2008;358:580–591.
- [10] Gerstein HC, Miller ME, Byington RP, Goff DC, Jr., Bigger JT, Buse JB, Cushman WC, Genuth S, Ismail-Beigi F, Grimm RH, Jr., Probstfield JL, Simons-Morton DG, Friedewald WT. Effects of intensive glucose lowering in type 2 diabetes. *N Engl J Med* 2008;358:2545–2559.
- [11] Duckworth W, Abraira C, Moritz T, Reda D, Emanuele N, Reaven PD, Zieve FJ, Marks J, Davis SN, Hayward R, Warren SR, Goldman S, McCarren M, Vitek ME, Henderson WG, Huang GD. Glucose control and vascular complications in veterans with type 2 diabetes. *N Engl J Med* 2009;360:129–139.
- [12] Ginsberg HN, Elam MB, Lovato LC, Crouse JR, 3rd, Leiter LA, Linz P, Friedewald WT, Buse JB, Gerstein HC, Probstfield J, Grimm RH, Ismail-Beigi F, Bigger JT, Goff DC, Jr., Cushman WC, Simons-Morton DG, Byington RP. Effects of combination lipid therapy in type 2 diabetes mellitus. *N Engl J Med* 2010;362:1563–1574.
- [13] Cushman WC, Evans GW, Byington RP, Goff DC, Jr., Grimm RH, Jr., Cutler JA, Simons-Morton DG, Basile JN, Corson MA, Probstfield JL, Katz L, Peterson KA, Friedewald WT, Buse JB, Bigger JT, Gerstein HC, Ismail-Beigi F. Effects of intensive blood-pressure control in type 2 diabetes mellitus. *N Engl J Med* 2010;362:1575–1585.
- [14] Ogawa S, Mori T, Nako K, Kato T, Takeuchi K, Ito S. Angiotensin II type 1 receptor blockers reduce urinary oxidative stress markers in hypertensive diabetic nephropathy. *Hypertension* 2006;47:699–705.

- [15] Galle J, Schwedhelm E, Pinnetti S, Boger RH, Wanner C. Antiproteinuric effects of angiotensin receptor blockers: telmisartan versus valsartan in hypertensive patients with type 2 diabetes mellitus and overt nephropathy. *Nephrol Dial Transplant* 2008;23:3174–3183.
- [16] Yasuda G, Kuji T, Hasegawa K, Ogawa N, Shimura G, Ando D, Umemura S. Safety and efficacy of fluvastatin in hyperlipidemic patients with chronic renal disease. *Ren Fail* 2004;26:411–418.
- [17] Matsuo S, Imai E, Horio M, Yasuda Y, Tomita K, Nitta K, Yamagata K, Tomino Y, Yokoyama H, Hishida A. Revised equations for estimated GFR from serum creatinine in Japan. *Am J Kidney Dis* 2009;53:982–992.
- [18] Tamura K, Tsurumi Y, Sakai M, Tanaka Y, Okano Y, Yamauchi J, Ishigami T, Kihara M, Hirawa N, Toya Y, Yabana M, Tokita Y, Ohnishi T, Umemura S. A possible relationship of nocturnal blood pressure variability with coronary artery disease in diabetic nephropathy. *Clin Exp Hypertens* 2007;29:31–42.
- [19] Tamura K, Yamauchi J, Tsurumi-Ikeya Y, Sakai M, Ozawa M, Shigenaga A, Azuma K, Okano Y, Ishigami T, Toya Y, Yabana M, Tokita Y, Ohnishi T, Umemura S. Ambulatory blood pressure and heart rate in hypertensives with renal failure: comparison between diabetic nephropathy and non-diabetic glomerulopathy. *Clin Exp Hypertens* 2008;30:33–43.
- [20] Kikuya M, Hozawa A, Ohokubo T, Tsuji I, Michimata M, Matsubara M, Ota M, Nagai K, Araki T, Satoh H, Ito S, Hisamichi S, Imai Y. Prognostic significance of blood pressure and heart rate variabilities: the Ohasama study. *Hypertension* 2000;36:901–906.
- [21] Sander D, Kukla C, Klingelhofner J, Winbeck K, Conrad B. Relationship between circadian blood pressure patterns and progression of early carotid atherosclerosis: A 3-year follow-up study. *Circulation* 2000;102:1536–1541.
- [22] Eto M, Toba K, Akishita M, Kozaki K, Watanabe T, Kim S, Hashimoto M, Aki J, Iijima K, Sudoh N, Yoshizumi M, Ouchi Y. Impact of blood pressure variability on cardiovascular events in elderly patients with hypertension. *Hypertens Res* 2005;28:1–7.
- [23] Mitsuhashi H, Tamura K, Yamauchi J, Ozawa M, Yanagi M, Dejima T, Wakui H, Masuda SI, Azuma K, Kanaoka T, Ohsawa M, Maeda A, Tsurumi-Ikeya Y, Okano Y, Ishigami T, Toya Y, Tokita Y, Ohnishi T, Umemura S. Effect of losartan on ambulatory short-term blood pressure variability and cardiovascular remodeling in hypertensive patients on hemodialysis. *Atherosclerosis* 2009;207:186–190.
- [24] Masuda S, Tamura K, Wakui H, Kanaoka T, Ohsawa M, Maeda A, Dejima T, Yanagi M, Azuma K, Umemura S. Effects of angiotensin II type 1 receptor blocker on ambulatory blood pressure variability in hypertensive patients with overt diabetic nephropathy. *Hypertens Res* 2009;32:950–955.
- [25] Ozawa M, Tamura K, Okano Y, Matsushita K, Ikeya Y, Masuda S, Wakui H, Dejima T, Shigenaga A, Azuma K, Ishigami T, Toya Y, Ishikawa T, Umemura S. Blood pressure variability as well as blood pressure level is important for left ventricular hypertrophy and brachial-ankle pulse wave velocity in hypertensives. *Clin Exp Hypertens* 2009;31:669–679.
- [26] Yamashina A, Tomiyama H, Takeda K, Tsuda H, Arai T, Hirose K, Koji Y, Hori S, Yamamoto Y. Validity, reproducibility, and clinical significance of noninvasive brachial-ankle pulse wave velocity measurement. *Hypertens Res* 2002;25:359–364.
- [27] Mancia G, Parati G. Ambulatory blood pressure monitoring and organ damage. *Hypertension* 2000;36:894–900.
- [28] Parati G, Di Rienzo T, Mancia G. Neural cardiovascular regulation and 24-hour blood pressure and heart rate variability. *Ann NY Acad Sci* 1996;783:47–63.
- [29] Shintani Y, Kikuya M, Hara A, Ohkubo T, Metoki H, Asayama K, Inoue R, Obara T, Aono Y, Hashimoto T, Hashimoto J, Totsum K, Hoshi H, Satoh H, Imai Y. Ambulatory blood pressure, blood pressure variability and the prevalence of carotid artery alteration: the Ohasama study. *J Hypertens* 2007;25:1704–1710.
- [30] Miao CY, Xie HH, Zhan LS, Su DF. Blood pressure variability is more important than blood pressure level in determination of end-organ damage in rats. *J Hypertens* 2006;24:1125–1135.
- [31] Kudo H, Kai H, Kajimoto H, Koga M, Takayama N, Mori T, Ikeda A, Yasuoka S, Aneawa T, Mifune H, Kato S, Hirooka Y, Imaizumi T. Exaggerated blood pressure variability superimposed on hypertension aggravates cardiac remodeling in rats via angiotensin II system-mediated chronic inflammation. *Hypertension* 2009;54:832–838.
- [32] Mancia G, Bombelli M, Facchetti R, Madotto F, Corrao G, Trevano FQ, Grassi G, Sega R. Long-term prognostic value of blood pressure variability in the general population: results of the Pressioni Arteriose Monitorate e Loro Associazioni Study. *Hypertension* 2007;49:1265–1270.
- [33] Pierdomenico SD, Di Nicola M, Esposito AL, Di Mascio R, Ballone E, Lapenna D, Cucurullo F. Prognostic value of different indices of blood pressure variability in hypertensive patients. *Am J Hypertens* 2009;22:842–847.
- [34] Rothwell PM, Howard SC, Dolan E, O'Brien E, Dobson JE, Dahloh B, Poulter NR, Sever PS. Effects of beta blockers and calcium-channel blockers on within-individual variability in blood pressure and risk of stroke. *Lancet Neurol* 2010;9:469–480.
- [35] Shigenaga A, Tamura K, Dejima T, Ozawa M, Wakui H, Masuda S, Azuma K, Tsurumi-Ikeya Y, Mitsuhashi H, Okano Y, Kokuho T, Sugano T, Ishigami T, Toya Y, Uchino K, Tokita Y, Umemura S. Effects of angiotensin II type 1 receptor blocker on blood pressure variability and cardiovascular remodeling in hypertensive patients on chronic peritoneal dialysis. *Nephron Clin Pract* 2009;112:c31–40.
- [36] Spallone V, Bernardi L, Ricordi L, Solda P, Maiello MR, Calciati A, Gambardella S, Fratino P, Menzinger G. Relationship between the circadian rhythms of blood pressure and sympathetic balance in diabetic autonomic neuropathy. *Diabetes* 1993;42:1745–1752.
- [37] Monteagudo PT, Nobrega JC, Cezarini PR, Ferreira SR, Kohlmann O, Jr., Ribeiro AB, Zanella MT. Altered blood pressure profile, autonomic neuropathy and nephropathy in insulin-dependent diabetic patients. *Eur J Endocrinol* 1996;135:683–688.
- [38] Ohkubo T, Imai Y, Tsuji I, Nagai K, Watanabe N, Minami N, Kato J, Kikuchi N, Nishiyama A, Aihara A, Sekino M, Satoh H, Hisamichi S. Relation between nocturnal decline in blood pressure and mortality. The Ohasama Study. *Am J Hypertens* 1997;10:1201–1207.
- [39] Nakano S, Fukuda M, Hotta F, Ito T, Ishii T, Kitazawa M, Nishizawa M, Kigoshi T, Uchida K. Reversed circadian blood pressure rhythm is associated with occurrences of both fatal and nonfatal vascular events in NIDDM subjects. *Diabetes* 1998;47:1501–1506.
- [40] Sturrock ND, George E, Pound N, Stevenson J, Peck GM, Sowter H. Non-dipping circadian blood pressure and renal impairment are associated with increased mortality in diabetes mellitus. *Diabet Med* 2000;17:360–364.
- [41] Kario K, Pickering TG, Matsuo T, Hoshida S, Schwartz JE, Shimada K. Stroke prognosis and abnormal nocturnal blood pressure falls in older hypertensives. *Hypertension* 2001;38:852–857.
- [42] Palmas W, Pickering TG, Teresi J, Schwartz JE, Moran A, Weinstock RS, Shea S. Ambulatory blood pressure monitoring and all-cause mortality in elderly people with diabetes mellitus. *Hypertension* 2009;53:120–127.
- [43] Eguchi K, Ishikawa J, Hoshida S, Pickering TG, Schwartz JE, Shimada K, Kario K. Night time blood pressure variability is a strong predictor for cardiovascular events in patients with type 2 diabetes. *Am J Hypertens* 2009;22:46–51.

- [44] Hou FF, Ren H, Owen WF, Jr., Guo ZJ, Chen PY, Schmidt AM, Miyata T, Zhang X. Enhanced expression of receptor for advanced glycation end products in chronic kidney disease. *J Am Soc Nephrol* 2004;15:1889–1896.
- [45] Nin JW, Jorsal A, Ferreira I, Schalkwijk CG, Prins MH, Parving HH, Tarnow L, Rossing P, Stehouwer CD. Higher Plasma Soluble Receptor for Advanced Glycation End Products (sRAGE) Levels Are Associated With Incident Cardiovascular Disease and All-Cause Mortality in Type 1 Diabetes: A 12-Year Follow-Up Study. *Diabetes* 2010;59:2027–2032.
- [46] Candido R, Forbes JM, Thomas MC, Thallas V, Dean RG, Burns WC, Tikellis C, Ritchie RH, Twigg SM, Cooper ME, Burrell LM. A breaker of advanced glycation end products attenuates diabetes-induced myocardial structural changes. *Circ Res* 2003;92:785–792.
- [47] Jandeleit-Dahm KA, Lassila M, Allen TJ. Advanced glycation end products in diabetes-associated atherosclerosis and renal disease: interventional studies. *Ann N Y Acad Sci* 2005;1043:759–766.
- [48] Jamerson K, Weber MA, Bakris GL, Dahlof B, Pitt B, Shi V, Hester A, Gupta J, Gatlin M, Velazquez EJ. Benazepril plus amlodipine or hydrochlorothiazide for hypertension in high-risk patients. *N Engl J Med* 2008;359:2417–2428.
- [49] Matsushita K, van der Velde M, Astor BC, Woodward M, Levey AS, de Jong PE, Coresh J, Gansevoort RT. Association of estimated glomerular filtration rate and albuminuria with all-cause and cardiovascular mortality in general population cohorts: a collaborative meta-analysis. *Lancet* 2010;375:2073–2081.
- [50] Bakris GL, Sarafidis PA, Weir MR, Dahlof B, Pitt B, Jamerson K, Velazquez EJ, Staikos-Byrne L, Kelly RY, Shi V, Chiang YT, Weber MA. Renal outcomes with different fixed-dose combination therapies in patients with hypertension at high risk for cardiovascular events (ACCOMPLISH): a prespecified secondary analysis of a randomised controlled trial. *Lancet* 2010;375:1173–1181.
- [51] Pop-Busui R, Evans GW, Gerstein HC, Fonseca V, Fleg JL, Hoogwerf BJ, Genuth S, Grimm RH, Corson MA, Prineas R. Effects of cardiac autonomic dysfunction on mortality risk in the Action to Control Cardiovascular Risk in Diabetes (ACCORD) trial. *Diabetes Care* 2010;33:1578–1584.
- [52] Winnicki M, Canali C, Accurso V, Dorigatti F, Giovinazzo P, Palatini P. Relation of 24-hour ambulatory blood pressure and short-term blood pressure variability to seasonal changes in environmental temperature in stage I hypertensive subjects. Results of the Harvest Trial. *Clin Exp Hypertens* 1996;18:995–1012.
- [53] Eguchi K, Hoshida S, Hoshida Y, Ishikawa S, Shimada K, Kario K. Reproducibility of ambulatory blood pressure in treated and untreated hypertensive patients. *J Hypertens* 2010;28:918–924.
- [54] di Rienzo M, Grassi G, Pedotti A, Mancia G. Continuous vs intermittent blood pressure measurements in estimating 24-hour average blood pressure. *Hypertension* 1983;5:264–269.
- [55] Thijs L, Staessen J, Fagard R, Zachariah P, Amery A. Number of measurements required for the analysis of diurnal blood pressure profile. *J Hum Hypertens* 1994;8:239–244.
- [56] Dolan E, O'Brien E. Blood pressure variability: clarity for clinical practice. *Hypertension* 2010;56:179–181.
- [57] Rothwell PM. Limitations of the usual blood-pressure hypothesis and importance of variability, instability, and episodic hypertension. *Lancet* 2010;375:938–948.
- [58] Stolarz-Skrzypek K, Thijs L, Richart T, Li Y, Hansen TW, Boggia J, Kuznetsova T, Kikuya M, Kawecka-Jaszcz K, Staessen JA. Blood pressure variability in relation to outcome in the International Database of Ambulatory blood pressure in relation to Cardiovascular Outcome: *Hypertens Res* 2010;33:757–766.

# Involvement of Runx3 in the basal transcriptional activation of the mouse angiotensin II type 1 receptor-associated protein gene

Miyuki Matsuda, Kouichi Tamura, Hiromichi Wakui, Toru Dejima, Akinobu Maeda, Masato Ohsawa, Tomohiko Kanaoka, Sona Haku, Kengo Azushima, Hiroko Yamasaki, Daisuke Saito, Tomonori Hirose, Yohei Maeshima, Yoji Nagashima and Satoshi Umemura

*Physiol. Genomics* 43:884-894, 2011. First published 17 May 2011;  
doi:10.1152/physiolgenomics.00005.2011

---

## You might find this additional info useful...

---

This article cites 36 articles, 26 of which can be accessed free at:

<http://physiolgenomics.physiology.org/content/43/14/884.full.html#ref-list-1>

Updated information and services including high resolution figures, can be found at:

<http://physiolgenomics.physiology.org/content/43/14/884.full.html>

Additional material and information about *Physiological Genomics* can be found at:

<http://www.the-aps.org/publications/pg>

---

This information is current as of May 19, 2012.

## Involvement of Runx3 in the basal transcriptional activation of the mouse angiotensin II type 1 receptor-associated protein gene

Miyuki Matsuda,<sup>1</sup> Kouichi Tamura,<sup>1</sup> Hiromichi Wakui,<sup>1</sup> Toru Dejima,<sup>1</sup> Akinobu Maeda,<sup>1</sup> Masato Ohsawa,<sup>1</sup> Tomohiko Kanaoka,<sup>1</sup> Sona Haku,<sup>1</sup> Kengo Azushima,<sup>1</sup> Hiroko Yamasaki,<sup>2</sup> Daisuke Saito,<sup>2</sup> Tomonori Hirose,<sup>3</sup> Yohei Maeshima,<sup>2</sup> Yoji Nagashima,<sup>4</sup> and Satoshi Umemura<sup>1</sup>

Departments of <sup>1</sup>Medical Science and Cardiorenal Medicine, <sup>3</sup>Molecular Biology, and <sup>4</sup>Molecular Pathology, Yokohama City University Graduate School of Medicine, Yokohama; and <sup>2</sup>Department of Medicine and Clinical Science, Okayama University Graduate School of Medicine, Dentistry and Pharmaceutical Sciences, Okayama, Japan

Submitted 4 January 2011; accepted in final form 16 May 2011

Matsuda M, Tamura K, Wakui H, Dejima T, Maeda A, Ohsawa M, Kanaoka T, Haku S, Azushima K, Yamasaki H, Saito D, Hirose T, Maeshima Y, Nagashima Y, Umemura S. Involvement of Runx3 in the basal transcriptional activation of the mouse angiotensin II type 1 receptor-associated protein gene. *Physiol Genomics* 43: 884–894, 2011. First published May 17, 2011; doi:10.1152/physiolgenomics.00005.2011.—We previously cloned a molecule that interacts with angiotensin II type 1 (AT1) receptor to exert an inhibitory function on AT1 receptor signaling that we named ATRAP/Agtrap (for AT1 receptor-associated protein). In the present study we examined the regulation of basal ATRAP gene expression using renal distal convoluted tubule cells. We found that serum starvation upregulated basal expression of ATRAP gene, a response that required de novo mRNA and protein synthesis. Luciferase assay revealed that the proximal promoter region directs transcription and that a putative binding site of runt-related transcription factors (RBE) is important for transcriptional activation. The results of RBE-decoy transfection and endogenous knockdown by small interference RNA showed that the runt-related transcription factor Runx3 is involved in ATRAP gene expression. Chromatin immunoprecipitation assay also supported the binding of Runx3 to the ATRAP promoter in renal distal convoluted tubule cells. Immunohistochemistry demonstrated the expression of Runx3 and ATRAP proteins in the distal convoluted and connecting tubules of the kidney in consecutive sections. Furthermore, the Runx3 immunostaining was decreased together with a concomitant suppression of ATRAP expression in the affected kidney after 7 days of unilateral ureteral obstruction. These findings indicate that Runx3 plays a role in ATRAP gene expression in renal distal tubular cells both in vitro and in vivo.

distal tubule; gene transcription; renin-angiotensin system; transcription regulation

ACTIVATION OF THE angiotensin II (ANG II) type 1 (AT1) receptor at local sites is involved in the pathogenesis of hypertension and the ensuing related target organ damages, as well as the development of renal inflammatory and fibrotic disease. We previously performed a yeast two-hybrid system screening of a murine kidney cDNA library and identified the molecule AT1 receptor-associated protein (ATRAP/Agtrap), which interacts specifically with the COOH-terminal cytoplasmic domain of the AT1 receptor (6, 17, 26). Previous in vitro studies using cardiovascular cells suggested that ATRAP promotes AT1 receptor internaliza-

tion and modulates the signaling pathways of the AT1 receptor (1, 10, 19, 28).

With respect to the tissue distribution and regulation of ATRAP expression in vivo, the ATRAP mRNA and protein are abundantly and widely distributed along the renal tubules, including the distal and proximal tubules (18, 29). We also demonstrated that there is a tissue-specific regulatory balancing of the expression of ATRAP and the AT1 receptor during the development of hypertension in rats (25). The activation of tissue ATRAP in transgenic models in which ATRAP expression was increased beyond baseline promoted ANG II-mediated internalization of the AT1 receptor (33) and abolished cardiac hypertrophy in response to ANG II stimulation (34). A recent study showed that a genetic deficiency of ATRAP in mice caused an enhanced surface expression of AT1 receptor in the kidney and an elevation of blood pressure through volume expansion (21). Therefore, it is important to elucidate the molecular mechanism of the tissue-specific regulation of ATRAP gene expression to determine the regulatory machinery for the tissue ATRAP level and/or ATRAP activity under both physiological and pathological conditions. Thus, as a first step, in this study we examined the basal transcriptional regulation of the ATRAP gene using mouse distal convoluted tubule cells (mDCT cells). These cells have been shown to have the phenotype of a polarized tight junction epithelium with morphologic and functional features retained from the parental cells (8, 22). The mDCT cells also express the endogenous AT1 receptor and ATRAP genes, as shown by reverse transcriptase-polymerase chain reaction (RT-PCR) and immunoblot analysis (18).

In the present study, we found that serum starvation upregulates basal ATRAP gene expression in renal DCT cells and that Runx3, one of the Runt-related transcription factors, is involved in the transcriptional activation of ATRAP gene expression. The Runt-related transcription factors have a conserved 128-amino acid Runt domain, a name derived from its homology to the pair-rule related gene “runt,” which plays a role in the segmented body patterning of *Drosophila* (5). The Runt-related transcription factors consist of Runx1, Runx2, and Runx3, and all three Runx proteins bind to the common DNA motif TGPYG-GTPy (Py is a pyrimidine), and each of these heterodimerizes with CBF $\beta$ , which makes no direct contact with DNA but, rather, increases DNA binding to Runx proteins.

Address for reprint requests and other correspondence: K. Tamura, Dept. of Medical Science and Cardiorenal Medicine, Yokohama City Univ. Graduate School of Medicine, 3-9 Fukuura, Kanazawa-ku, Yokohama 236-0004, Japan (e-mail: tamukou@med.yokohama-cu.ac.jp).

**MATERIALS AND METHODS**

This study was performed in accordance with the National Institutes of Health guidelines for the use of experimental animals. All of the animal studies were reviewed and approved by the Animal Studies Committee of Yokohama City University.

**Cell culture.** The mDCT cells were kindly provided by Dr. Peter A. Friedman (University of Pittsburgh School of Medicine, Pittsburgh, PA). The cells had been previously isolated and functionally characterized as described (9, 22).

**Animals and treatment.** Adult C57BL/6 mice were purchased from Oriental Yeast Kogyo (Tokyo, Japan). The procedure of unilateral ureteral obstruction (UUO) was performed using C57BL/6 mice as described previously (23). Briefly, with the mice under anesthesia, the left ureter was ligated at two locations. Mice that were operated on were killed under anesthesia 7 days after UUO. Sham operation was also performed, in which the ureters were manipulated but not ligated.

**Immunoblot analysis.** Characterization and specificity of the anti-mouse ATRAP antibody have been described (23, 28, 29). The

total membrane fraction was isolated using a Plasma Membrane Protein Extraction Kit (BioVision) according to the manufacturer's protocol. Immunoblot analysis was performed as described previously (23, 28, 29, 31, 34), and the images were analyzed quantitatively using a FUJI LAS3000 Image Analyzer (FUJI Film, Tokyo, Japan) for determination of the ATRAP protein levels.

**Plasmid construction and transcriptional ATRAP promoter assay.** The *KpnI/BamHI* fragment of the 374-bp mouse ATRAP promoter (−302 to +72 of the putative transcriptional start site) was amplified from C57BL/6J genomic DNA using the pair of primers in Table 1. Construction of mutations in the Runx-binding element (RBE) and SMAD-binding element (SBE) was performed by oligonucleotide (ODN)-directed mutagenesis (11, 13, 27). The sequences of the ODN used to create the mutated SBE (SBE-mt) and mutated RBE (RBE-mt) are shown in Table 1. To normalize transfection efficiency, we employed the Dual-Luciferase Assay System (Promega) as described previously (22).

**Transfection of decoy ODN and small interfering RNA.** The sequences of the decoy ODN against RBE and control HA ODN are

Table 1. Primer sequences used in the study

Primers	Primer Sequences
<i>Construction of wild-type and mutated ATRAP promoter-containing plasmids</i>	
Wild-type ATRAP promoter	
forward	5'-gggggtacCTTGTGCAAGGGAAGTAAGA-3'
reverse	5'-cgggataccGAACTCGGAACAACTTCCT-3'
SBE-mt	
forward	5'-AGAGAGGATGTTCTGGGCCTCCACCAACTGTTACCACACCCGAG-3'
reverse	5'-CTGCGGGTGTGGTAACAGTTGGTGGAGGCCAGAACATCCTCTCT-3'
RBE-mt	
forward	5'-TGGGCAGACACCAACTGTTAGTGTACCCGAGTTTCTGCCGGCTT-3'
reverse	5'-AAGCGGGCAGAAACTGCGGTTACACTAACAGTTGGTGTCTGCCCA-3'
<i>Transfection of decoy ODN</i>	
RBE-decoy ODN	5'-CTCGTCTACGACATGCACCGT-3' and 5'-ACGGTGCATGTGGTAGACGAG-3'
HA-decoy ODN	5'-CCATACGATGTTCCAGATTAC-3' and 5'-GGTATGCTACAAGGTCTAATG-3'
<i>Transfection of siRNA</i>	
siRunx1	
sense	5'-ccgucuuuacaaaucggcTT-3'
antisense	5'-ggcggauuuuguaaagacggTG-3'
siRunx2	
sense	5'-cgaauaggcagcagcucuuAA-3'
antisense	5'-aaugcgugcugccauucAG-3'
siRunx3	
sense	5'-uucacgaccuucgauucTG-3'
antisense	5'-cgaaucgaaggucguugaaCC-3'
siHA	
sense	5'-ccauacgauguuccagauuAC-3'
antisense	5'-aaucuggaacaucguauGGT-3'
<i>Real-time RT-PCR analysis</i>	
Runx1	
forward	5'-TAGCGAGATTCAACGACCTC-3'
reverse	5'-GTGGCGGATTTGTAAGACG-3'
Runx2	
forward	5'-GTACTTCGTGAGCATCCTAT-3'
reverse	5'-AGCGTGCTGCCATTCGAGGT-3'
Runx3	
forward	5'-GGTTCAACGACCTTCGATTG-3'
reverse	5'-GGTTGGTGAACACGGTGATT-3'
<i>Chromatin immunoprecipitation assay</i>	
forward	5'-TCCTCTCCAACCTCACTTTT-3'
reverse	5'-TAACAGTTGGTGTCTGCCCA-3'

ATRAP, AT1 receptor-associated protein; SBE, SMAD-binding element; mt, mutated; RBE, Runx-binding element; HA, hemagglutinin; ODN, oligonucleotide; siRNA, small interfering RNA.

shown in Table 1. To knockdown the endogenous expression of Runx proteins with small interfering RNA (siRNA), siRunx1, siRunx2, and siRunx3 primers were synthesized (Table 1). As a negative control, siHA primers were also synthesized. The annealed double-strand decoy ODN (100 nM) or siRNA (2.5–10 nM) was introduced into mDCT cells using Lipofectamine RNAiMAX (Invitrogen).

**Real-time quantitative RT-PCR analysis.** Total RNA was extracted and purified using the RNeasy Kit (QIAGEN), and real-time quantitative RT-PCR analysis was performed as described previously (34). The detection primer sequences for Runx1, Runx2, and Runx3 are shown in Table 1.

**Co-immunoprecipitation.** Kidneys were minced, homogenized in reaction buffer (20 mM HEPES, 150 mM NaCl, 1 mM EDTA, 1%

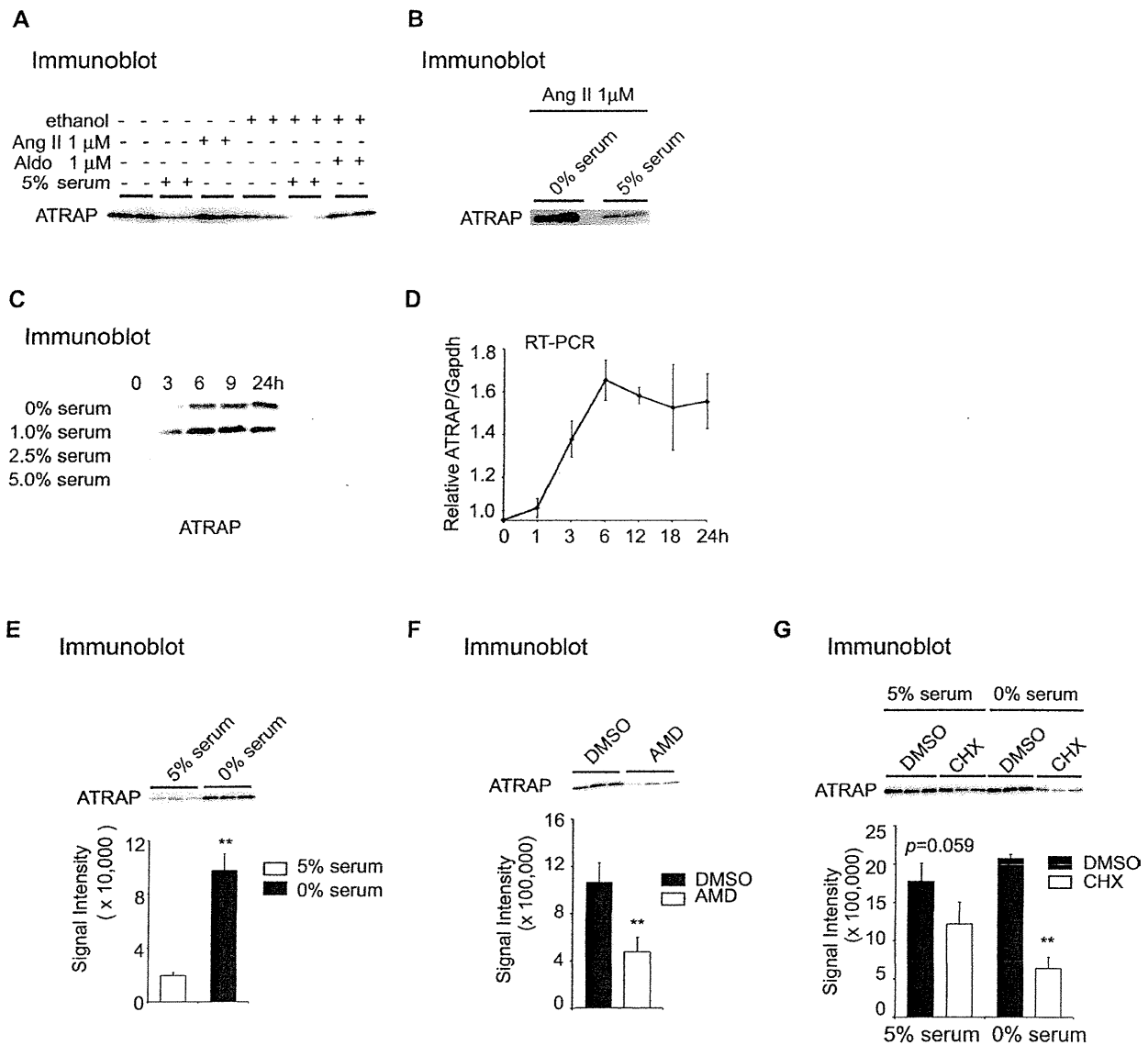


Fig. 1. Serum deprivation-mediated regulation of basal AT1 receptor-associated protein (ATRAP) expression involves the activation of transcription and translation in mouse distal convoluted tubule (mDCT) cells. **A**: representative immunoblot showing the effects of 24-h treatment with ANG II (1  $\mu$ M), aldosterone (Aldo, 1  $\mu$ M), or serum (5%) on ATRAP protein expression in whole mDCT extracts after serum starvation for 24 h. Ethanol (final concentration 0.1%) was used as a solvent for aldosterone. **B**: representative immunoblot showing the effects of 24-h treatment with ANG II (1  $\mu$ M) with or without serum (5%) on ATRAP protein expression in whole mDCT extracts after serum starvation for 24 h. **C**: representative immunoblot showing the time- and concentration-dependent effects of serum starvation for the indicated times on relative ATRAP protein expression in whole mDCT extracts. **D**: quantitative real-time RT-PCR analysis showing time-dependent effects of serum starvation on the relative ATRAP mRNA levels. RNA quantity was normalized to the signal generated by constitutively expressed Gapdh and is expressed relative to those achieved with extracts at baseline (0 h) ( $n = 3$ ). **E**: immunoblot showing the effects of 24-h serum deprivation (5% serum -) on ATRAP protein expression in the total membrane fraction of mDCT cells ( $n = 3$ ). **\*\*** $P < 0.01$ , vs. nondeprived cells (5% serum +). **F**: immunoblot showing the effects of actinomycin D (AMD, 1  $\mu$ g/ml) on 6-h serum deprivation-mediated expression of ATRAP expression in the total membrane fraction of mDCT cells ( $n = 3$ ). **\*\*** $P < 0.01$ , vs. vehicle-treated cells (AMD-, DMSO). **G**: immunoblot showing the effects of 6-h treatment of cycloheximide (CHX, 10  $\mu$ g/ml) on ATRAP protein expression in the total membrane fraction of the serum deprived (0% serum) or nondeprived (5% serum) mDCT cells ( $n = 3$ ). **\*\*** $P < 0.01$ , vs. vehicle-treated cells (CHX-, DMSO). Immunodetection of the membrane stained by Coomassie blue dye served as an internal control for the determination of equal protein loading.

NP-40, 1 mM DTT, and protease inhibitors), and centrifuged at 3,000 g for 30 min. Then, the solubilized proteins were subjected to absorption by protein G-beads to avoid a nonspecific reaction. For immunoprecipitation, anti-PY antibody (clone 6B4, MBL) cross-linked protein G-beads with Bis (sulfosuccinimidyl) suberate (#21580 Thermo Fisher Scientific) were used. Immunoblotting was performed using anti-Runx3 antibody (AV37263, Sigma-Aldrich).

**Chromatin immunoprecipitation assay.** Chromatin immunoprecipitation (ChIP) assay with anti-Runx3 antibody or normal rabbit IgG was performed using the detection primers in Table 1, essentially according to the manufacturer's protocol (Active Motif) (2, 15). Briefly, mDCT cells transiently transfected with the wild-type or mutated ATRAP promoter-containing plasmids were treated with paraformaldehyde to cross-link the protein-DNA complexes. Then, cell lysates were sonicated to reduce the DNA fragments to an average size of ~500 bp. Following immunoprecipitation with anti-Runx3 antibody or normal rabbit IgG as control, DNA was purified from the antibody-bound and unbound fractions, and enrichment of the ATRAP promoter sequences in the bound fraction was assayed by the overlap extension PCR method (13).

**Immunohistochemistry.** Immunohistochemistry was performed essentially as described previously (23, 29). The sections were incubated with anti-RUNX3 antibody (H-50, sc-30197; Santa Cruz Biotechnology, Santa Cruz, CA) diluted at 1:50. For the study of specific nephron markers, the sections were incubated with 1) aquaporin 2 antibody (#178612, Calbiochem), 2) calbindin D-28K antibody (C2724, Sigma-Aldrich), or 3) Tamm-Horsfall glycoprotein antibody (sc-20631, Santa Cruz Biotechnology).

**Statistical analysis.** Data are expressed as the means ± SD. Statistical significance was determined using unpaired Student's *t*-test or analysis of variance followed by Bonferroni test, with *P* < 0.05 considered statistically significant.

**RESULTS**

**Serum deprivation-mediated regulation of ATRAP expression involves the activation of transcription and translation in mDCT cells.** To examine whether external stimuli exert an influence on the expression of the ATRAP gene in mDCT cells, we first assessed the effects of various vasoactive substances by immunoblot analysis, such as ANG II and aldosterone, on ATRAP protein expression. After mDCT cells were incubated with serum-free medium for 24 h, mDCT cells were incubated with the indicated medium for an additional 24 h. Although treatment with ANG II (1 μM) or aldosterone (1 μM) did not significantly affect ATRAP protein expression, the expression was markedly decreased after exposure of the cells to 5% serum (Fig. 1A). This inhibitory effect of serum on basal ATRAP expression was not affected by costimulation with ANG II (Fig. 1B). These results show that serum is a dominant inhibitor of ATRAP gene expression in mDCT cells.

To determine whether serum starvation increased ATRAP gene expression, we examined the time course of ATRAP protein expression in mDCT cells treated with various concentrations of serum. Expression of the ATRAP protein started to increase 3 h after treatment with 0 or 1.0% serum and peaked at 6 h, and at 24 h the level was still elevated compared with baseline, while treatment with 2.5 or 5% serum did not affect ATRAP protein expression (Fig. 1C). The results of real-time quantitative RT-PCR analysis showed that the serum starvation-induced increase in ATRAP protein expression was accompanied by an activation of ATRAP mRNA expression (Fig. 1D), indicating transcription plays a role in the basal expression of the ATRAP gene.

ATRAP is predicted to have three transmembrane domains (6, 17), so we also examined the effect of serum starvation on basal ATRAP protein expression using the total cellular membrane fraction. The results showed that serum starvation increased the basal ATRAP protein expression in the membrane

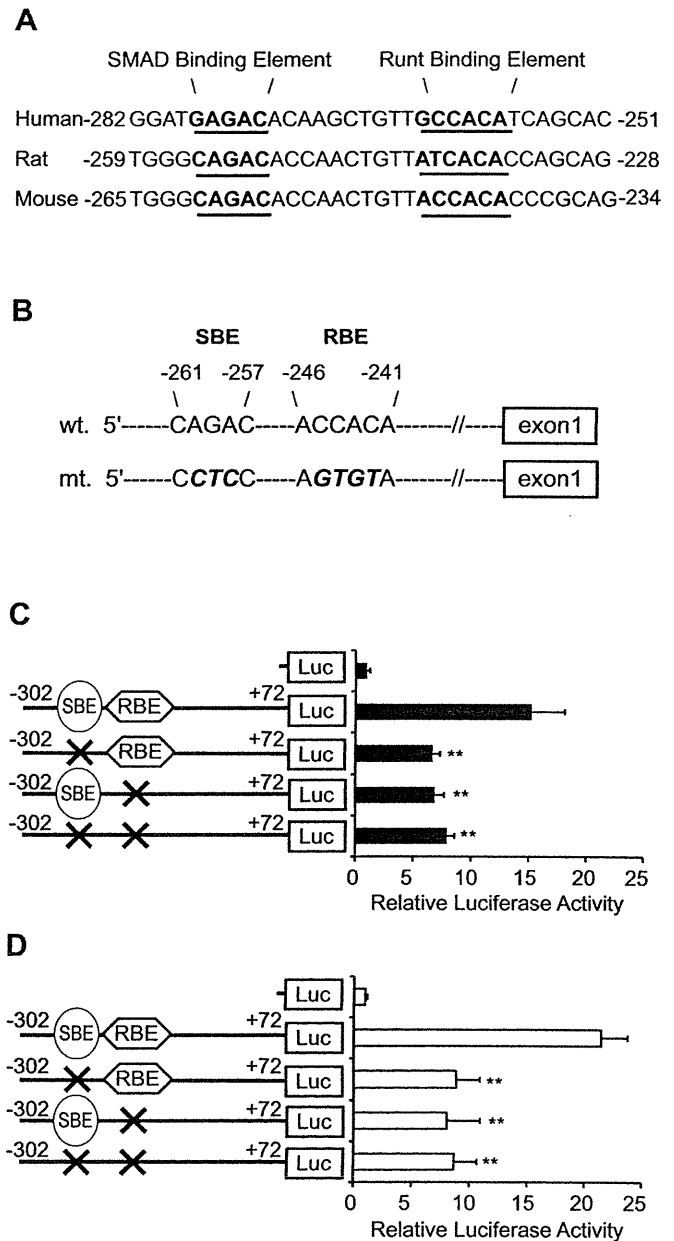


Fig. 2. The Runx binding element (RBE) and SMAD binding element (SBE) are important for transcriptional activation of the ATRAP promoter in mDCT cells. A: sequences of the SBE and RBE in the proximal promoter regions of the human, rat, and mouse ATRAP genes. B: construction of site-directed mutations in the SBE and RBE in the mouse ATRAP promoter sequence. Wild-type sequences (wt.) and mutated sequences (mt.) are shown. Effects of mutations in the SBE and RBE on the transcriptional activity of the mouse ATRAP promoter (-302 to +72 of the transcriptional start site)-luciferase hybrid gene in serum containing (C, 5% serum) or deprived (D, 0% serum) mDCT cells. The relative luciferase activities were calculated relative to those achieved with the promoterless control plasmid (n = 3). \*\**P* < 0.01, vs. wild-type sequences.



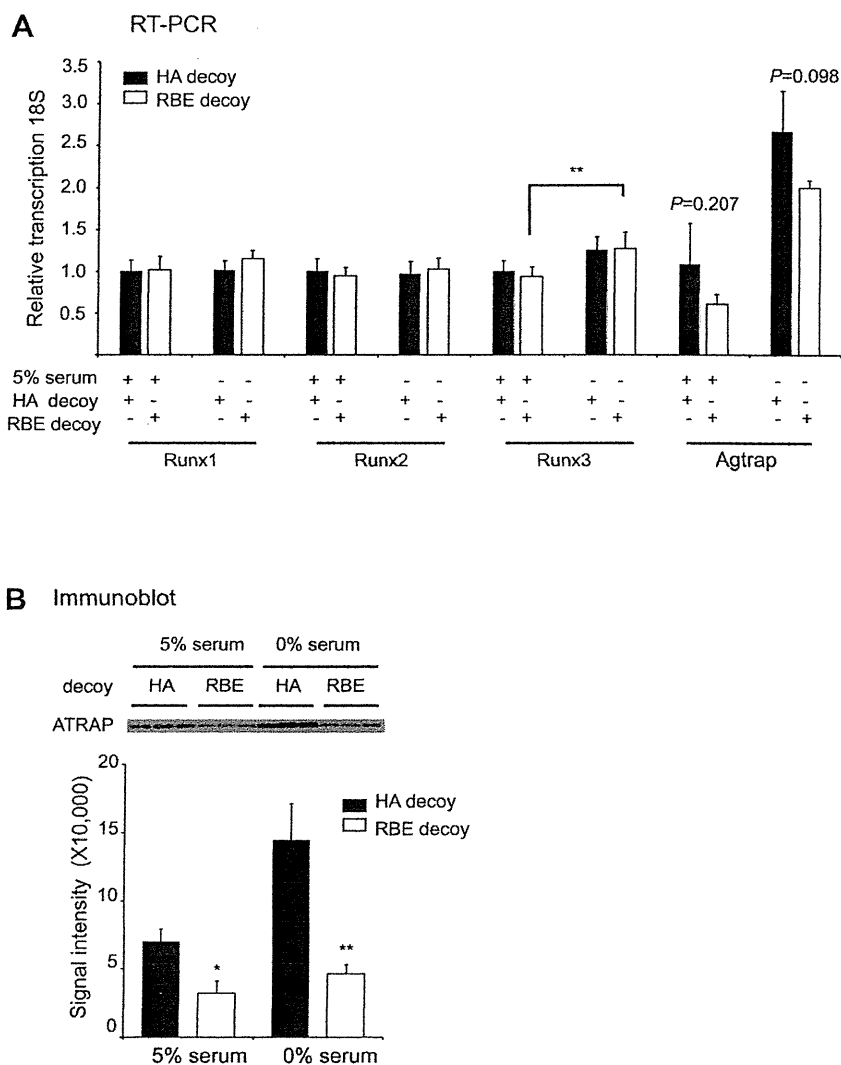
fraction as well (Fig. 1E), and membrane fraction extracts were used for the analysis of ATRAP protein expression thereafter. Next, to determine whether de novo RNA or protein synthesis was required for the starvation-induced increase in basal ATRAP expression, mDCT cells were treated with actinomycin D or cycloheximide and incubated for 6 h in the presence or absence of 5% serum. The RNA synthesis inhibitor actinomycin D (Fig. 1F), as well as the protein synthesis inhibitor cycloheximide (Fig. 1G), significantly suppressed the starvation-mediated increase in basal ATRAP protein expression. These results demonstrate that both de novo mRNA transcription and de novo protein synthesis are required for the upregulation of basal ATRAP expression by serum starvation.

*The SMAD and Runx binding elements are important for the transcriptional activation of the ATRAP promoter in mDCT cells.* The above results suggest that activation of transcription may play an important role in the serum starvation-induced upregulation of basal ATRAP expression in mDCT cells. The entire mouse ATRAP locus spanning 11002 nt on chromosome 4 consists of 5 exons (32). The first exon is 148 bp in length and contains 121 bp of untranslated nucleotides upstream of the

initiating ATG. Sequence analysis of the 5'-flanking region of the ATRAP gene using the TF Search program and Signal Scan algorithm revealed the absence of a TATA box and the presence of a GC-rich region extending >200 nt from the initiating methionine. The percentage of GC dinucleotides in this region ranged between 65 and 80%, with a CG:GC ratio of 0.94, thus fulfilling the length and base composition criteria for a canonical CpG island (32).

Analysis of the proximal promoter region made up of approximately -300 bp of the putative transcriptional start site of the ATRAP gene, with the MOTIF Search program (<http://motif.genome.jp/>), showed the presence of a putative SBE and Runx binding site (RBE), which are highly conserved among the mouse, rat, and human forms (Fig. 2A). To examine the functional role of these conserved elements in the regulation of ATRAP gene transcription, we mutated the core binding sequences of SBE and RBE in the endogenous mouse ATRAP promoter by PCR-directed mutagenesis (Fig. 2B). Although the proximal promoter region from -302 to +72 of the putative transcriptional start site of the ATRAP gene exhibited substantial transcriptional activity, site-directed mutations of either SBE or

Fig. 3. RBE decoy decreases endogenous ATRAP gene expression in mDCT cells. **A:** quantitative real-time RT-PCR analysis showing the effects of RBE-decoy transfection on the relative mRNA levels of Runx1, Runx2, Runx3, and ATRAP. RNA quantity was normalized to the signal generated by the constitutively expressed 18S ribosomal RNA and expressed relative to extracts derived from nondeprived mDCT cells transfected with control hemagglutinin (HA) decoy (5% serum +, HA-decoy +) ( $n = 3$ ). \* $P < 0.05$ , vs. HA, hemagglutinin; decoy; \*\* $P < 0.01$ , vs. HA decoy. **B:** immunoblot showing the effects of RBE-decoy transfection on ATRAP protein expression in the total membrane fraction of the serum deprived (0% serum) or nondeprived (5% serum) mDCT cells ( $n = 3$ ). HA decoy was used as a control. Immunodetection membrane stained by Coomassie blue dye served as an internal control for the determination of equal protein loading. \*\* $P < 0.01$ , vs. HA decoy.



RBE significantly decreased the transcriptional activity in serum containing (Fig. 2C) or deprived (Fig. 2D) mDCT cells.

*Runx3 is involved in the upregulation of endogenous ATRAP gene expression in mDCT cells.* To inhibit the binding of the runt-related transcription factors (Runx1, Runx2, and Runx3) to RBE, we performed transient transfection studies using a decoy ODN method that has been well described (7, 20). A double-stranded decoy ODN was transfected into mDCT cell cultures to interfere with Runx binding to RBE, and the effects on the endogenous expression of Runx and ATRAP were subsequently analyzed. The results of real-time quantitative RT-PCR analysis showed that the ATRAP mRNA level had a

tendency of decrease as the result of RBE-decoy transfection despite there being no apparent change in the expression of Runx mRNA (Fig. 3A). Interestingly, serum starvation upregulated Runx3 mRNA levels, and this upregulation was not affected by RBE-decoy transfection (Fig. 3A). Furthermore, transfection with the RBE-decoy ODN decreased the serum starvation-induced upregulation of the ATRAP protein levels in mDCT cells (Fig. 3B). These results indicate that Runx binding sites are involved in the transcriptional activation of ATRAP gene by serum starvation in mDCT cells.

To further determine which Runx protein is responsible for the serum starvation-induced activation of ATRAP expression

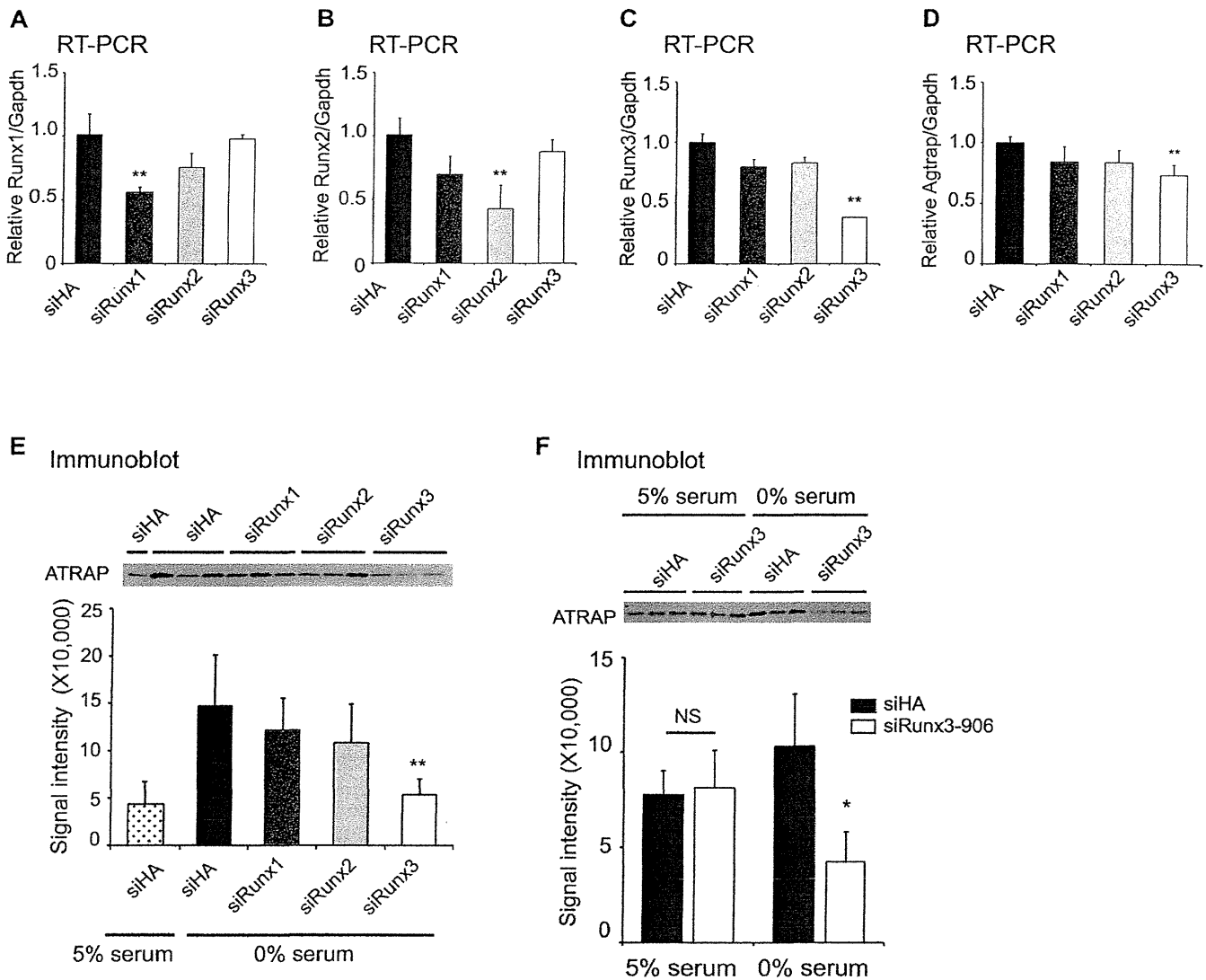


Fig. 4. Specific knockdown of Runx3 by small interference (si) RNA decreases endogenous ATRAP gene expression in mDCT cells. Quantitative real-time RT-PCR analysis showing the effects of respective siRNAs transfection on the relative Runx1 (A), Runx2 (B), and Runx3 (C) mRNA levels. RNA quantity was normalized to the signal generated by constitutively expressed GAPDH and is expressed relative to those achieved with extracts derived from mDCT cells transfected with control siHA ( $n = 3$ ).  $**P < 0.01$ , vs. siHA. D: quantitative real-time RT-PCR analysis showing the effects of respective siRNA transfection on the relative ATRAP mRNA level. RNA quantity was normalized to the signal generated by constitutively expressed GAPDH and expressed relative to those achieved with extracts derived from mDCT cells transfected with control siHA ( $n = 3$ ).  $**P < 0.01$ , vs. siHA. E: immunoblot showing the effects of respective siRNA transfection on ATRAP protein expression in the total membrane fraction of the deprived (0% serum) mDCT cells ( $n = 3$ ). siHA was used as a control.  $**P < 0.01$ , vs. siHA transfected into the deprived mDCT cells. F: immunoblot showing the effects of respective siRNA transfection on ATRAP protein expression in the total membrane fraction of the serum containing (5% serum) or deprived (0% serum) mDCT cells ( $n = 3$ ). siHA was used as a control.  $*P < 0.05$ , vs. siHA. Immunodetection of the membrane stained by Coomassie blue dye served as an internal control for the determination of equal protein loading.

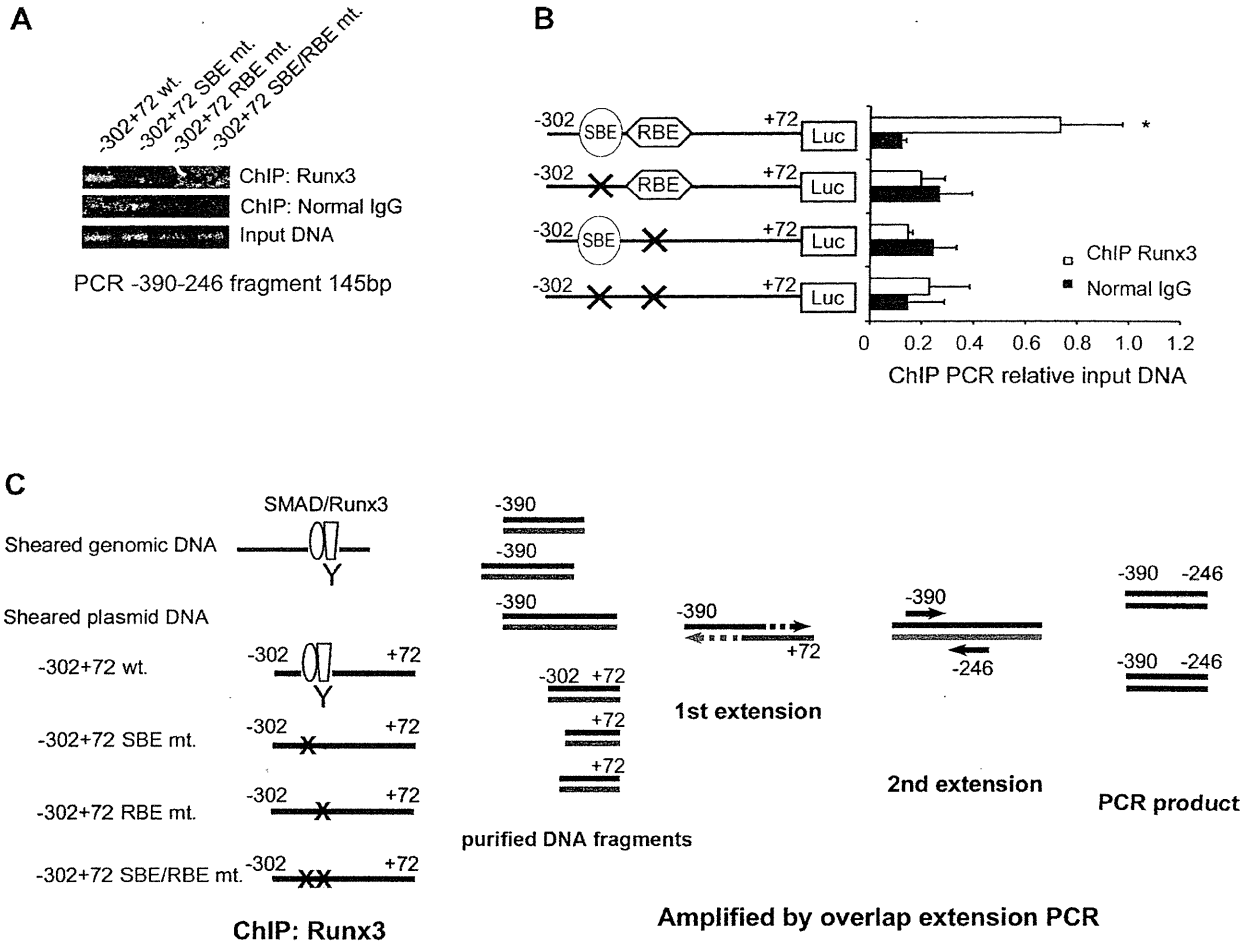


Fig. 5. Runx3 specifically binds to the ATRAP promoter in mDCT cells in ChIP assay. *A*: representative ethidium bromide staining showing the amplified ATRAP promoter fragment of 145 bp containing SBE and RBE in the anti-Runx3 antibody-bound immunoprecipitates in the mDCT cells, which were transiently transfected with the wild-type or mutated ATRAP promoter (–302 to +72)-luciferase hybrid genes, on 3% agarose gel. *B*: quantitative real-time PCR analysis showing a specific enrichment of the ATRAP promoter fragment containing wild-type SBE and RBE in the anti-Runx3 antibody-bound immunoprecipitates. The relative values of enrichment were calculated relative to the input DNA ( $n = 3$ ). Normal IgG was used as a control.  $*P < 0.05$ , vs. normal IgG. *C*: schematic explanation of the overlap extension PCR detection in the ChIP assay. Briefly, mDCT cells transiently transfected with the wild-type or mutated ATRAP promoter-containing plasmids were treated with paraformaldehyde to cross-link the protein-DNA complexes. Cell lysates were sonicated to reduce the DNA fragments to an average size of ~500 bp. Following immunoprecipitation with anti-Runx3 antibody or normal rabbit IgG, DNA was purified from the antibody-bound and unbound fractions, and the enrichment of the ATRAP promoter fragment in the bound fraction was assayed by the overlap extension PCR method. The overlap extension PCR analysis was performed using the forward primer (–390), which anneals to genomic DNA, and the reverse primer (–246), which anneals to both genomic and plasmid DNA.

in mDCT cells, we examined the effect of Runx siRNA transfection on endogenous ATRAP gene expression. The mRNA levels of Runx1 (Fig. 4A), Runx2 (Fig. 4B), and Runx3 (Fig. 4C) were significantly decreased after transfection with their

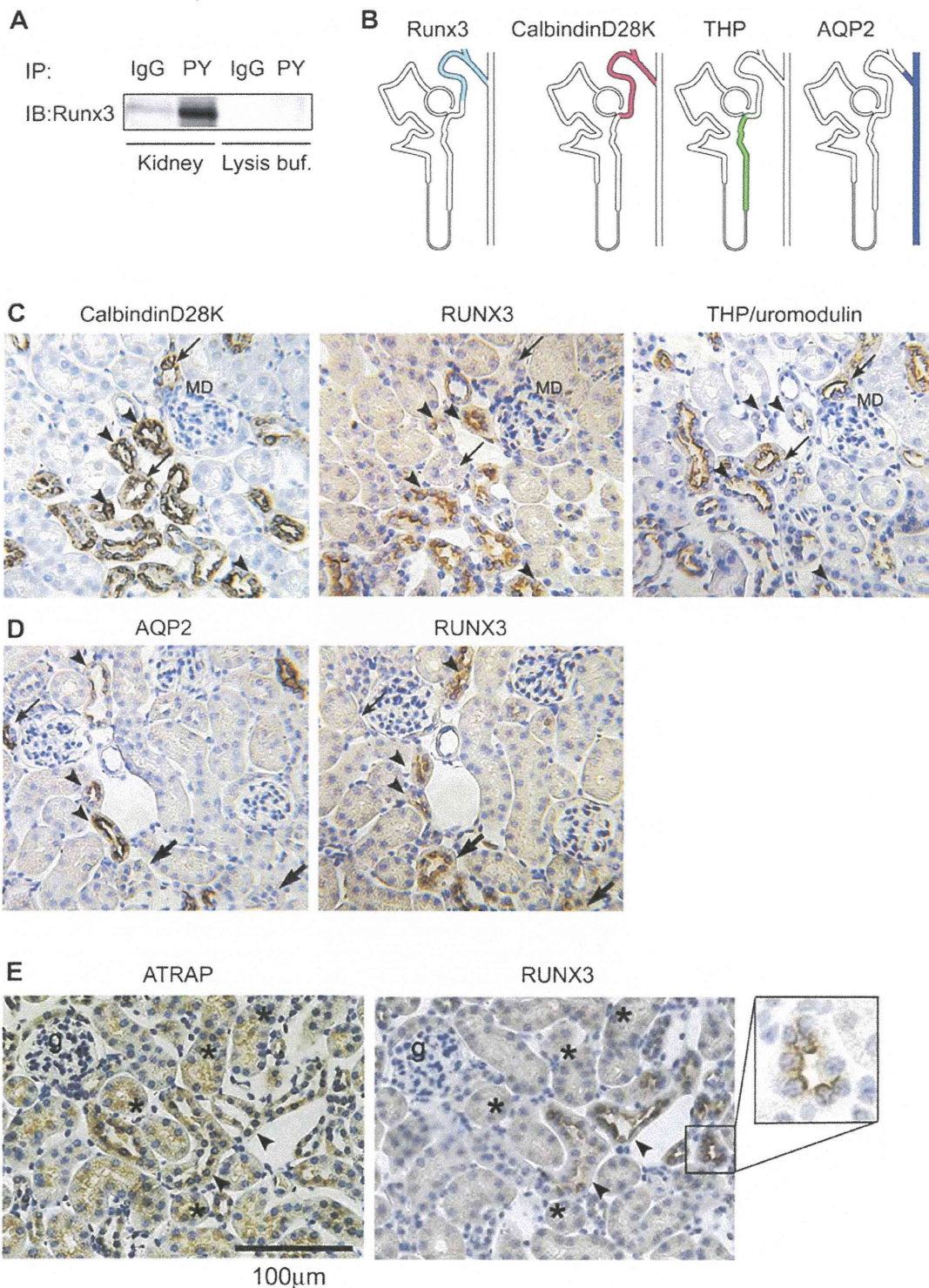
respective siRNA in serum-starved mDCT cells. Importantly, among these Runx siRNAs, only the siRNA reduction of Runx3 resulted in a significant decrease in the levels of ATRAP mRNA (Fig. 4D). Furthermore, Runx3 knockdown caused a significant

Fig. 6. Runx3 immunostaining is observed mainly in the DCT and connecting tubules of the mouse kidney, and the Runx3-immunopositive (IP) distal tubules expressed the ATRAP protein. *A*: immunoblot (IB) showing that the anti-Runx3-specific antibody recognized the apparent molecular mass of the major band as ~44 kDa, which was consistent with the predicted molecular mass in the mouse kidney extracts immunoprecipitated using the anti-PY motif antibody (PY, kidney), compared with the control normal IgG (IgG, kidney). *B*: schematic localization of Runx3, CalbindinD28K, Tamm-Horsfall protein (THP) and aquaporin 2 (AQP2) along the nephron segments. *C*: consecutive sections showing the immunostaining of CalbindinD28K, Runx3, and THP, respectively. The distal tubules immunopositive for all of the CalbindinD28K, Runx3, and THP immunostaining are designated by arrowheads, and those positive for CalbindinD28K and THP, but not for Runx3, are designated by arrows. MD, macula densa. *D*: consecutive sections showing the immunostaining of aquaporin 2 (AQP2) and Runx3, respectively. The distal tubules immunopositive for both the AQP2 and Runx3 immunostaining are designated by arrowheads, while those positive for AQP2 but not for Runx3 are designated by thin arrows, and those positive for Runx3, but not for AQP2, are designated by thick arrows. *E*: consecutive sections showing the immunostaining of ATRAP and Runx3, respectively. The distal tubules immunopositive for both ATRAP and Runx3 are designated by arrowheads, with Runx3 immunostaining at a higher magnification shown on the right. Scale bars indicate 100  $\mu\text{m}$ . g, Glomerulus; \*proximal convoluted tubules. Original magnification:  $\times 400$ .

suppression of the serum starvation-induced upregulation of ATRAP protein expression (Fig. 4E), while the inhibitory effect of Runx3 knockdown on ATRAP expression was not observed in the serum-containing mDCT cells (Fig. 4F).

ChIP assays were also performed to examine the association of Runx3 with the ATRAP promoter (Fig. 5). The mDCT cells

were transiently transfected with the wild-type or mutated ATRAP promoter (-302 to +72)-luciferase hybrid genes, which were the same constructs as used in the promoter assays in (Fig. 2). The immunoprecipitates obtained by cross-linking ChIP assay were subjected to overlap extension PCR analysis using the forward primer (-390), which anneals to genomic



DNA, and the reverse primer (−246), which anneals to both genomic and plasmid DNAs. The ChIP assay results support a direct interaction of Runx3 with the ATRAP promoter in mDCT cells. Notably, since mutations of either SBE or RBE significantly decreased the occupancy of the ATRAP promoter by Runx3, neither Runx3 nor SMAD by itself is sufficient, and a combinatorial interaction of Runx3 and SMAD appears to be necessary for the efficient binding of Runx3 to the ATRAP promoter.

*Runx3 is expressed mainly in the DCT and CNT in the mouse kidney.* While we previously demonstrated that ATRAP is highly expressed in the mouse kidney (29) and other studies have shown that Runx3 is abundantly expressed in epithelial cells of the gastrointestinal tract (4, 14), there is no report of Runx3 expression in the mouse kidney. Thus, we examined endogenous Runx3 protein expression in the kidney of adult C57BL/6J mice. The Runx proteins share a common COOH-terminal PY-motif, and immunoprecipitation using an anti-PY motif antibody and the mouse kidney extracts followed by immunoblot analysis revealed that the anti-Runx3-specific antibody recognized an apparent molecular mass of ~44 kDa, which was consistent with the predicted molecular mass (Fig. 6A).

We then examined Runx3 protein distribution in normal adult mouse kidneys sections by immunohistochemistry. We found the Runx3 immunostaining sites to be localized to renal tubules in the cortex, with no involvement of the medulla or papilla (data not shown). To identify the specific tubular segments in the Runx3 immunostaining, consecutive sections were stained for Runx3 and markers specific to the tubular segments (Fig. 6B). We used a specific antibody against calbindin-D, a calcium-binding protein that is expressed primarily in the DCT and connecting tubules (CNT) (16, 30), and Runx3 protein immunoreactivity was observed specifically in the calbindin-D positive distal tubules (DCT and CNT) other than the macula densa (Fig. 6C, calbindinD28K and Runx3). We also used a polyclonal antibody against the Tamm-Horsfall protein that is expressed in the thick ascending limbs of the loop of Henle, and a polyclonal antibody against aquaporin 2, which is specifically expressed in the collecting tubules. Runx3 immunostaining was not detected in the Tamm-Horsfall protein-positive tubules (Fig. 6C, Runx3 and THP/uromodulin, arrow) and was detected only weakly in the early portion of the distal tubules, which were positive for both calbindin-D and Tamm-Horsfall protein (Fig. 6C, calbindinD28K, Runx3, and THP/uromodulin, arrowhead). Runx3 immunostaining was largely absent in the aquaporin 2-positive tubules (Fig. 6D, AQP2 and Runx3, arrow) and when evident was only partially observed (Fig. 6D, AQP2 and Runx3, arrowhead). There was no significant Runx3 staining in the glomeruli, proximal tubules, collecting ducts, or vasculature including the arcuate artery, interlobular arteries, and arterioles (data not shown).

We investigated whether ATRAP and Runx3 are coexpressed in the same tubular segment. In consecutive sections stained for ATRAP and Runx3, all of the Runx3-immunopositive distal tubules expressed ATRAP (Fig. 6E, ATRAP and Runx3, arrowhead), indicating partial coexpression of Runx3 with ATRAP in the distal tubules (DCT and CNT) of the mouse kidney. With respect to the intracellular distribution of Runx3 in the distal tubular cells (DCT and CNT), the staining of Runx3 was intense in the perinuclear and cytosolic region on

the apical side at higher magnification (Fig. 6E, Runx3). Finally, we examined the effects of UUO on Runx3 and ATRAP expression. ATRAP mRNA expression was significantly downregulated in the affected kidney after 7 days of UUO, with a concomitant decrease in ATRAP immunostaining (Fig. 7, A and B). On the other hand, while the Runx3 mRNA expression was upregulated in the affected kidney after 7 days of UUO, the distal tubules were not immunopositive for Runx3 (Fig. 7, A and B).

## DISCUSSION

Serum starvation in this study was found to be a major positive regulator of ATRAP gene expression in mDCT cells. Serum

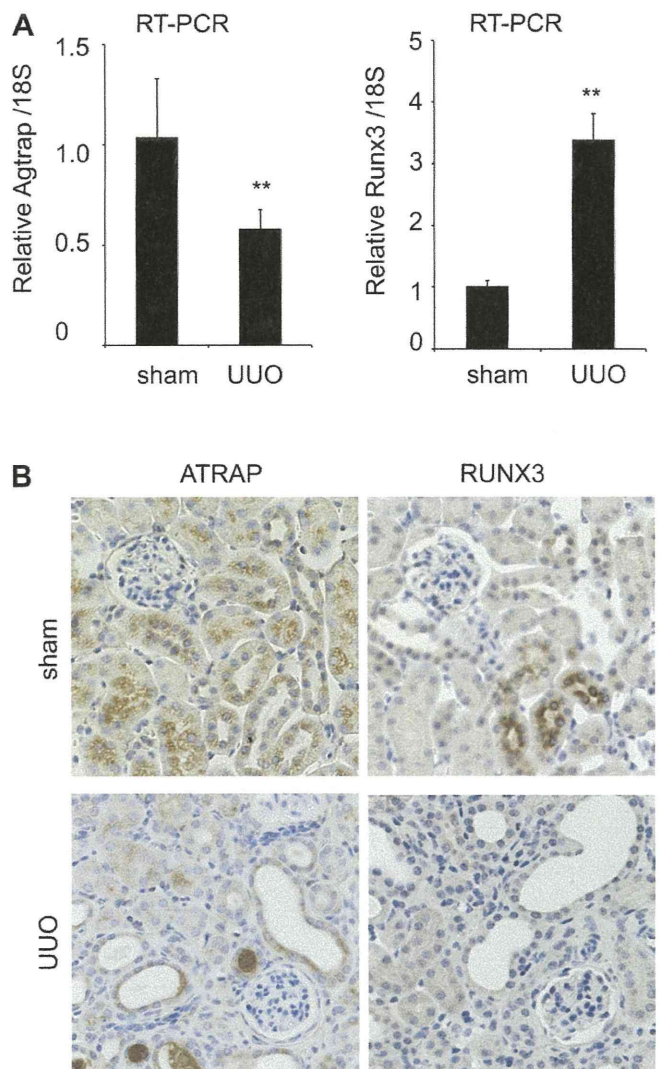


Fig. 7. Regulation of ATRAP and Runx3 mRNA and protein expression in the affected kidney by unilateral ureteral obstruction (UUO). A: quantitative real-time RT-PCR analysis showing the effects of UUO on the relative ATRAP and Runx3 mRNA levels. RNA quantity was normalized to the signal generated by the constitutively expressed 18S rRNA and is expressed relative to those achieved with extracts derived from sham-operated kidney ( $n = 3$ ).  $***P < 0.01$ , vs. sham. B: consecutive sections showing the effects of UUO on the immunostains of ATRAP and Runx3 in the affected kidney. Original magnification:  $\times 400$ .

starvation is known to reduce cellular proliferation and induce differentiation in cultured cells, including renal tubule cells (3), and this may include increased ATRAP expression in mDCT cells. Since the starvation-induced increase in basal ATRAP expression was inhibited by treatment with either actinomycin D or cycloheximide (Fig. 1, *F* and *G*), it is likely that the serum starvation induced activation of basal ATRAP expression involves de novo mRNA and protein synthesis. Sequence analysis of the 5'-flanking region of the ATRAP gene using the TF Search program and Signal Scan algorithm revealed the absence of a TATA box and the presence of a GC-rich region extending >200 nt from the initiating methionine. The percentage of GC dinucleotides in this region ranged between 65 and 80%, with a CG:GC ratio of 0.94, thus fulfilling the length and base composition criteria for a canonical CpG island specifically located at the transcriptional start site (32).

The results of the transient transfection assay demonstrate that the proximal promoter region from -302 to +72 of the ATRAP gene is sufficient to drive luciferase reporter gene expression in deprived mDCT cells. Mutation of either SBE or RBE significantly decreased the promoter activity of the ATRAP gene, but a mutation of both SBE and RBE did not further decrease the promoter activity in the transfection assay (Fig. 2). Similarly, mutations of SBE or RBE alone or together significantly decreased the binding of Runx3 to the ATRAP promoter to a similar extent in the ChIP assay (Fig. 5). These results suggest that the combinatorial interaction of SBE and RBE is important for the binding of Runx3 to the ATRAP promoter and transcriptional activation of the proximal promoter of the ATRAP gene by Runx3. This is consistent with previous studies showing that the intranuclear targeting of the Runx-Smad complex to transcriptionally active SBE and RBE adjacent sites is necessary for transcriptional regulation by Runx and SMAD proteins (12, 37). A previous study also reported a similar coordinated action of SMAD and Runx3 drives the transcription of the *GL $\gamma$ 2b* gene in response to TGF $\beta$ 1 stimulation (24).

With respect to the functional role of Runx3 in the expression of the ATRAP gene, the results of the RBE-decoy transfection experiment and Runx siRNA-mediated endogenous Runx knock-down assay indicate that it is Runx3 among the Runx family transcription factors that is critically involved in the activation of ATRAP gene expression. Interestingly, multiple RBEs are present throughout the mouse ATRAP locus, including both the coding and noncoding regions (data not shown). A previous study showed that Runx2 directly regulated ribosomal biogenesis through multiple RBEs in the ribosomal RNA locus by DNA binding and indirectly by affecting chromatin histone modification (36). The results of the present study indicate that the direct DNA binding of Runx3 to RBE is involved in the activation of ATRAP gene expression in mDCT cells, but further studies are needed to elucidate the molecular mechanism of Runx3-mediated transcriptional activation of the ATRAP gene promoter.

The Runx3 gene is reported to be expressed in the mesenchymal elements; it controls the proper development of gastric endothelial cells by apoptosis and also acts as a tumor suppressor gene (5). In this study, we showed that *in vitro* Runx3 as well as ATRAP is expressed in mDCT cells and, *in vivo*, in the distal tubules of the mouse kidney. To the best of our knowledge, this is the first report demonstrating that Runx3 is expressed in renal tubular cells. Furthermore, the intrarenal localization of Runx3 does not completely coincide with that of

ATRAP in terms of the tubular segments. While the expression of the Runx3 protein was mainly localized in the DCT and CNT of the distal tubules, the ATRAP protein was widely distributed along the renal tubules (3, 29).

Our previous studies showed that the intracellular localization of ATRAP also does not completely coincide with that of the AT1 receptor, the binding partner of ATRAP, in the tubular segments (29). The results of *in vitro* experiments showed that ANG II treatment induces substantial colocalization of ATRAP and AT1 receptor in cardiovascular cells (1, 28), thereby suggesting that ATRAP and the AT1 receptor can have other effectors, as reported (10). Therefore, the results of the present study suggest that there are other factor(s), such as coactivator(s), which cooperate with both Runx3 and ATRAP. Further molecular screens for both Runx3 and ATRAP are needed to identify such putative additional partners for these molecules, which may act cooperatively or independently in terms of timing and specific cellular locations in the kidney.

Finally, UUO is a well-established experimental model of progressive tubulointerstitial fibrosis. UUO leads to changes in renal hemodynamics, inflammatory responses in the kidney, and tubular hypertrophy and interstitial fibrosis of the affected kidney (23). The renin-angiotensin system is also known to be activated in UUO, and the results of the present study showed a significant downregulation of Runx3 and ATRAP expression in the affected kidney, suggesting a possible role of Runx3 in the regulation of ATRAP *in vivo*.

The limitations of the present study include the lack of data on the effect of serum starvation on ATRAP binding to the AT1 receptor and its subsequent internalization. Further studies are needed to elucidate the function of ATRAP on AT1 receptor signaling under starvation conditions, and these will be taken up in due course. Caution should be used in interpreting the finding of this study in terms of the pathophysiology in humans, and further studies are warranted to investigate the role of Runx3 in ATRAP regulation under various physiological and/or pathological conditions.

In summary, the results of the present study demonstrate the Runx3-mediated basal transcriptional activation of ATRAP gene in renal distal tubular cells is dependent on its DNA binding. Furthermore, the results of immunohistochemical analysis show a partial colocalization of Runx3 and ATRAP proteins in the distal tubules of the mouse kidney. These findings suggest an interesting molecular link between Runx3, one of the important Runx-related transcription factors in the determination of cell lineage and differentiation (35), and ATRAP, a newly emerging component of the renin-angiotensin system, a link that is likely to play a role in the regulation of ATRAP gene expression in the renal distal tubules.

#### ACKNOWLEDGMENTS

We are indebted to Dr. P. Friedman (University of Pittsburgh School of Medicine, Pittsburgh, PA) for providing us with the mDCT cells. The authors also thank Emi Maeda and Hiroko Morinaga for technical assistance and helpful discussion. Pacific Edit reviewed the manuscript prior to submission.

#### GRANTS

This work was supported in part by grants from the Japanese Ministry of Education, Science, Sports, and Culture; by a Health and Labor Sciences Research grant; and by Salt Science Research Foundation Grants 1033, 1134; the Kidney Foundation, Japan (JKFB11-25); and Strategic Research Project of Yokohama City University.

## DISCLOSURES

No conflicts of interest, financial or otherwise, are declared by the author(s).

## REFERENCES

- Azuma K, Tamura K, Shigenaga A, Wakui H, Masuda S, Tsurumi-Ikeya Y, Tanaka Y, Sakai M, Matsuda M, Hashimoto T, Ishigami T, Lopez-Ilasaca M, Umemura S. Novel regulatory effect of angiotensin II type 1 receptor-interacting molecule on vascular smooth muscle cells. *Hypertension* 50: 926–932, 2007.
- Carabana J, Ortigoza E, Krangel MS. Regulation of the murine Ddelta2 promoter by upstream stimulatory factor 1, Runx1, and c-Myb. *J Immunol* 174: 4144–4152, 2005.
- Carraro-Lacroix LR, Ramirez MA, Zorn TM, Reboucas NA, Malnic G. Increased NHE1 expression is associated with serum deprivation-induced differentiation in immortalized rat proximal tubule cells. *Am J Physiol Renal Physiol* 291: F129–F139, 2006.
- Chuang LS, Ito Y. RUNX3 is multifunctional in carcinogenesis of multiple solid tumors. *Oncogene* 29: 2605–2615, 2010.
- Cohen MM Jr. Perspectives on RUNX genes: an update. *Am J Med Genet A* 149A: 2629–2646, 2009.
- Daviet L, Lehtonen JY, Tamura K, Griese DP, Horiuchi M, Dzau VJ. Cloning and characterization of ATRAP, a novel protein that interacts with the angiotensin II type 1 receptor. *J Biol Chem* 274: 17058–17062, 1999.
- Ehsan A, Mann MJ, Dell'Acqua G, Tamura K, Braun-Dullaes R, Dzau VJ. Endothelial healing in vein grafts: proliferative burst unimpaired by genetic therapy of neointimal disease. *Circulation* 105: 1686–1692, 2002.
- Friedman PA, Gesek FA. Stimulation of calcium transport by amiloride in mouse distal convoluted tubule cells. *Kidney Int* 48: 1427–1434, 1995.
- Gesek FA, Friedman PA. Sodium entry mechanisms in distal convoluted tubule cells. *Am J Physiol Renal Fluid Electrolyte Physiol* 268: F89–F98, 1995.
- Guo S, Lopez-Ilasaca M, Dzau VJ. Identification of calcium-modulating cyclophilin ligand (CAML) as transducer of angiotensin II-mediated nuclear factor of activated T cells (NFAT) activation. *J Biol Chem* 280: 12536–12541, 2005.
- Higuchi R, Krummel B, Saiki RK. A general method of in vitro preparation and specific mutagenesis of DNA fragments: study of protein and DNA interactions. *Nucleic Acids Res* 16: 7351–7367, 1988.
- Javed A, Bae JS, Afzal F, Gutierrez S, Pratap J, Zaidi SK, Lou Y, van Wijnen AJ, Stein JL, Stein GS, Lian JB. Structural coupling of Smad and Runx2 for execution of the BMP2 osteogenic signal. *J Biol Chem* 283: 8412–8422, 2008.
- Kuipers OP, Boot HJ, de Vos WM. Improved site-directed mutagenesis method using PCR. *Nucleic Acids Res* 19: 4558, 1991.
- Li QL, Ito K, Sakakura C, Fukamachi H, Inoue K, Chi XZ, Lee KY, Nomura S, Lee CW, Han SB, Kim HM, Kim WJ, Yamamoto H, Yamashita N, Yano T, Ikeda T, Itohara S, Inazawa J, Abe T, Hagiwara A, Yamagishi H, Ooe A, Kaneda A, Sugimura T, Ushijima T, Bae SC, Ito Y. Causal relationship between the loss of RUNX3 expression and gastric cancer. *Cell* 109: 113–124, 2002.
- Lim M, Zhong C, Yang S, Bell AM, Cohen MB, Roy-Burman P. Runx2 regulates survivin expression in prostate cancer cells. *Lab Invest* 90: 222–233, 2010.
- Loffing-Cueni DFS, Sauter D, Daidie D, Siegrist N, Meneton P, Staub O, Loffing J. Dietary sodium intake regulates the ubiquitin-protein ligase Nedd4–2 in the renal collecting system. *J Am Soc Nephrol* 17: 1264–1274, 2006.
- Lopez-Ilasaca M, Liu X, Tamura K, Dzau VJ. The angiotensin II type I receptor-associated protein, ATRAP, is a transmembrane protein and a modulator of angiotensin II signaling. *Mol Biol Cell* 14: 5038–5050, 2003.
- Masuda S, Tamura K, Wakui H, Maeda A, Dejima T, Hirose T, Toyoda M, Azuma K, Ohsawa M, Kanaoka T, Yanagi M, Yoshida SI, Mitsuhashi H, Matsuda M, Ishigami T, Toya Y, Suzuki D, Nagashima Y, Umemura S. Expression of angiotensin II Type 1 receptor interacting molecule in normal human kidney and IgA nephropathy. *Am J Physiol Renal Physiol* 299: F720–F731, 2010.
- Min LJ, Mogi M, Tamura K, Iwanami J, Sakata A, Fujita T, Tsukuda K, Jing F, Iwai M, Horiuchi M. Angiotensin II type 1 receptor-associated protein prevents vascular smooth muscle cell senescence via inactivation of calcineurin/nuclear factor of activated T cells pathway. *J Mol Cell Cardiol* 47: 798–809, 2009.
- Morishita R, Higaki J, Tomita N, Aoki M, Moriguchi A, Tamura K, Murakami K, Kaneda Y, Ogihara T. Role of transcriptional cis-elements, angiotensinogen gene-activating elements, of angiotensinogen gene in blood pressure regulation. *Hypertension* 27: 502–507, 1996.
- Oppermann M, Gess B, Schweda F, Castrop H. Atrap deficiency increases arterial blood pressure and plasma volume. *J Am Soc Nephrol* 21: 468–477, 2010.
- Sakai M, Tamura K, Tsurumi Y, Tanaka Y, Koide Y, Matsuda M, Ishigami T, Yabana M, Tokita Y, Hiroi Y, Komuro I, Umemura S. Expression of MAK-V/Hunk in renal distal tubules and its possible involvement in proliferative suppression. *Am J Physiol Renal Physiol* 292: F1526–F1536, 2007.
- Satoh M, Kashiwara N, Yamasaki Y, Maruyama K, Okamoto K, Maeshima Y, Sugiyama H, Sugaya T, Murakami K, Makino H. Renal interstitial fibrosis is reduced in angiotensin II type 1a receptor-deficient mice. *J Am Soc Nephrol* 12: 317–325, 2001.
- Seo GY, Park SR, Kim PH. Analyses of TGF-beta1-inducible Ig germline gamma2b promoter activity: involvement of Smads and NF-kappaB. *Eur J Immunol* 39: 1157–1166, 2009.
- Shigenaga A, Tamura K, Wakui H, Masuda S, Azuma K, Tsurumi-Ikeya Y, Ozawa M, Mogi M, Matsuda M, Uchino K, Kimura K, Horiuchi M, Umemura S. Effect of olmesartan on tissue expression balance between angiotensin II receptor and its inhibitory binding molecule. *Hypertension* 52: 672–678, 2008.
- Tamura K, Tanaka Y, Tsurumi Y, Azuma K, Shigenaga A, Wakui H, Masuda S, Matsuda M. The role of angiotensin AT1 receptor-associated protein in renin-angiotensin system regulation and function. *Curr Hypertens Rep* 9: 121–127, 2007.
- Tamura K, Tanimoto K, Ishii M, Murakami K, Fukamizu A. Proximal and core DNA elements are required for efficient angiotensinogen promoter activation during adipogenic differentiation. *J Biol Chem* 268: 15024–15032, 1993.
- Tanaka Y, Tamura K, Koide Y, Sakai M, Tsurumi Y, Noda Y, Umemura M, Ishigami T, Uchino K, Kimura K, Horiuchi M, Umemura S. The novel angiotensin II type 1 receptor (AT1R)-associated protein ATRAP downregulates AT1R and ameliorates cardiomyocyte hypertrophy. *FEBS Lett* 579: 1579–1586, 2005.
- Tsurumi Y, Tamura K, Tanaka Y, Koide Y, Sakai M, Yabana M, Noda Y, Hashimoto T, Kihara M, Hirawa N, Toya Y, Kiuchi Y, Iwai M, Horiuchi M, Umemura S. Interacting molecule of AT1 receptor, ATRAP, is colocalized with AT1 receptor in the mouse renal tubules. *Kidney Int* 69: 488–494, 2006.
- Vekaria RM, Shirley DG, Sevigny J, Unwin RJ. Immunolocalization of ectonucleotidases along the rat nephron. *Am J Physiol Renal Physiol* 290: F550–F560, 2006.
- Vila-Carriles WH, Kovacs GG, Jovov B, Zhou ZH, Pahwa AK, Colby G, Esmail O, Gillespie GY, Mapstone TB, Markert JM, Fuller CM, Bubien JK, Benos DJ. Surface expression of ASIC2 inhibits the amiloride-sensitive current and migration of glioma cells. *J Biol Chem* 281: 19220–19232, 2006.
- Wakaguri H, Yamashita R, Suzuki Y, Sugano S, Nakai K. DBTSS: database of transcription start sites, progress report 2008. *Nucleic Acids Res* 36: D97–D101, 2008.
- Wakui H, Tamura K, Matsuda M, Bai Y, Dejima T, Shigenaga AI, Masuda S, Azuma K, Maeda A, Hirose T, Ishigami T, Toya Y, Yabana M, Minamisawa S, Umemura S. Intrarenal suppression of angiotensin II type 1 receptor binding molecule in angiotensin II-infused mice. *Am J Physiol Renal Physiol* 299: F991–F1003, 2010.
- Wakui H, Tamura K, Tanaka Y, Matsuda M, Bai Y, Dejima T, Masuda S, Shigenaga A, Maeda A, Mogi M, Ichihara N, Kobayashi Y, Hirawa N, Ishigami T, Toya Y, Yabana M, Horiuchi M, Minamisawa S, Umemura S. Cardiac-specific activation of angiotensin II type 1 receptor-associated protein completely suppresses cardiac hypertrophy in chronic angiotensin II-infused mice. *Hypertension* 55: 1157–1164, 2010.
- Walrad PB, Hang S, Joseph GS, Salas J, Gergen JP. Distinct contributions of conserved modules to runt transcription factor activity. *Mol Biol Cell* 21: 2315–2326, 2010.
- Young DW, Hassan MQ, Pratap J, Galindo M, Zaidi SK, Lee SH, Yang X, Xie R, Javed A, Underwood JM, Furciniti P, Imbalzano AN, Penman S, Nickerson JA, Montecino MA, Lian JB, Stein JL, van Wijnen AJ, Stein GS. Mitotic occupancy and lineage-specific transcriptional control of rRNA genes by Runx2. *Nature* 445: 442–446, 2007.
- Zaidi SK, Sullivan AJ, van Wijnen AJ, Stein JL, Stein GS, Lian JB. Integration of Runx and Smad regulatory signals at transcriptionally active subnuclear sites. *Proc Natl Acad Sci USA* 99: 8048–8053, 2002.

**Hiromichi Wakui, Kouichi Tamura, Miyuki Matsuda, Yunzhe Bai, Toru Dejima, Atsu-ichiro Shigenaga, Shin-ichiro Masuda, Koichi Azuma, Akinobu Maeda, Tomonori Hirose, Tomoaki Ishigami, Yoshiyuki Toya, Machiko Yabana, Susumu Minamisawa and Satoshi Umemura**

*Am J Physiol Renal Physiol* 299:991-1003, 2010. First published Aug 25, 2010;  
doi:10.1152/ajprenal.00738.2009

**You might find this additional information useful...**

---

This article cites 50 articles, 36 of which you can access free at:

<http://ajprenal.physiology.org/cgi/content/full/299/5/F991#BIBL>

Updated information and services including high-resolution figures, can be found at:

<http://ajprenal.physiology.org/cgi/content/full/299/5/F991>

Additional material and information about *AJP - Renal Physiology* can be found at:

<http://www.the-aps.org/publications/ajprenal>

---

This information is current as of November 21, 2010 .



## Intrarenal suppression of angiotensin II type 1 receptor binding molecule in angiotensin II-infused mice

Hiromichi Wakui,<sup>1\*</sup> Kouichi Tamura,<sup>1\*</sup> Miyuki Matsuda,<sup>1</sup> Yunzhe Bai,<sup>2</sup> Toru Dejima,<sup>1</sup> Atsu-ichiro Shigenaga,<sup>1</sup> Shin-ichiro Masuda,<sup>1</sup> Koichi Azuma,<sup>1</sup> Akinobu Maeda,<sup>1</sup> Tomonori Hirose,<sup>3</sup> Tomoaki Ishigami,<sup>1</sup> Yoshiyuki Toya,<sup>1</sup> Machiko Yabana,<sup>1</sup> Susumu Minamisawa,<sup>4</sup> and Satoshi Umemura<sup>1</sup>

<sup>1</sup>Department of Medical Science and Cardiorenal Medicine, <sup>2</sup>Cardiovascular Research Institute, and <sup>3</sup>Department of Molecular Biology, Yokohama City University Graduate School of Medicine, Yokohama; and <sup>4</sup>Department of Life Science and Medical Bio-science, Waseda University, Tokyo, Japan

Submitted 28 December 2009; accepted in final form 23 August 2010

Wakui H, Tamura K, Matsuda M, Bai Y, Dejima T, Shigenaga A, Masuda S, Azuma K, Maeda A, Hirose T, Ishigami T, Toya Y, Yabana M, Minamisawa S, Umemura S. Intrarenal suppression of angiotensin II type 1 receptor binding molecule in angiotensin II-infused mice. *Am J Physiol Renal Physiol* 299: F991–F1003, 2010. First published August 25, 2010; doi:10.1152/ajprenal.00738.2009.—ATRAP [ANG II type 1 receptor (AT1R)-associated protein] is a molecule which directly interacts with AT1R and inhibits AT1R signaling. The aim of this study was to examine the effects of continuous ANG II infusion on the intrarenal expression and distribution of ATRAP and to determine the role of AT1R signaling in mediating these effects. C57BL/6 male mice were subjected to vehicle or ANG II infusions at doses of 200, 1,000, or 2,500 ng·kg<sup>-1</sup>·min<sup>-1</sup> for 14 days. ANG II infusion caused significant suppression of ATRAP expression in the kidney but did not affect ATRAP expression in the testis or liver. Although only the highest ANG II dose (2,500 ng·kg<sup>-1</sup>·min<sup>-1</sup>) provoked renal pathological responses, such as an increase in the mRNA expression of angiotensinogen and the  $\alpha$ -subunit of the epithelial sodium channel, ANG II-induced decreases in ATRAP were observed even at the lowest dose (200 ng·kg<sup>-1</sup>·min<sup>-1</sup>), particularly in the outer medulla of the kidney, based on immunohistochemical staining and Western blot analysis. The decrease in renal ATRAP expression by ANG II infusion was prevented by treatment with the AT1R-specific blocker olmesartan. In addition, the ANG II-mediated decrease in renal ATRAP expression through AT1R signaling occurred without an ANG II-induced decrease in plasma membrane AT1R expression in the kidney. On the other hand, a transgenic model increase in renal ATRAP expression beyond baseline was accompanied by a constitutive reduction of renal plasma membrane AT1R expression and by the promotion of renal AT1R internalization as well as the decreased induction of angiotensinogen gene expression in response to ANG II. These results suggest that the plasma membrane AT1R level in the kidney is modulated by intrarenal ATRAP expression under physiological and pathophysiological conditions in vivo.

gene expression; renin-angiotensin system; angiotensin; receptor; hypertension

in linking receptor-mediated signal transduction to the specific pathophysiological response to ANG II (16, 41). The AT1R-associated protein (ATRAP), which is a molecule specifically interacting with the carboxyl-terminal domain of the AT1R, was cloned using a yeast-two-hybrid screening system (8, 21). The results of previous in vitro studies and ATRAP transgenic mice studies showed that ATRAP suppresses ANG II-mediated pathological responses in cardiovascular cells and tissues by promoting the constitutive internalization of AT1R (1, 7, 11, 30, 40, 44), thereby suggesting ATRAP to be an endogenous inhibitor of AT1R signaling (22, 37).

With respect to the tissue distribution and regulation of ATRAP expression in vivo, ATRAP and AT1R are broadly expressed in many tissues, including the kidney, and there is a tissue-specific regulatory balancing of the expression of ATRAP and AT1R during the development of hypertension in spontaneously hypertensive rats (35). Chronic infusion of ANG II is one of the representative models of hypertension and end-organ damage and is associated with the activation of the intrarenal renin-angiotensin system, including upregulation of renal angiotensinogen through the AT1R pathway (10, 20, 49). Furthermore, previous studies using a series of kidney cross-transplant experiments also showed that the activation of intrarenal AT1R is required for the development of ANG II-dependent hypertension and the related end-organ damage (5, 6). Thus we hypothesized that the intrarenal distribution and regulation of endogenous ATRAP expression may also be involved in the pathophysiological responses to ANG II. Accordingly, studies were performed to examine the changes in intrarenal ATRAP expression during ANG II infusion in mice and to determine the role of AT1R in mediating these responses. Furthermore, we examined whether the plasma membrane AT1R level was influenced by the ANG II-mediated decrease in the renal ATRAP level and/or by an increase in the renal ATRAP level in a transgenic model, to analyze the relationship between ATRAP and AT1R expression in the kidney.

### METHODS

**Materials.** ANG II was purchased from Sigma. The AT1R-specific blocker olmesartan (RNH6270) was kindly supplied by Daiichi-Sankyo Pharmaceuticals (Tokyo, Japan).

**Animals and ANG II infusion.** Adult male C57BL/6 mice (10–12 wk of age, Oriental Yeast Kogyo) were divided into three groups ( $n = 6–8$  mice/group) for the subcutaneous infusion of vehicle or ANG II (either 200, 1,000, or 2,500 ng·kg<sup>-1</sup>·min<sup>-1</sup>) via an osmotic minipump (ALZA) for 14 days. The percentage of body weight increase (% BW increase) was calculated as follows: % BW increase = [(BW at day 14) – (BW at baseline) × 100]/(BW at baseline). In several of the experiments, vehicle or olmesartan (10 mg·kg<sup>-1</sup>·day<sup>-1</sup>) in the

EVIDENCE SUGGESTS THAT THE activation of angiotensin II (ANG II) type 1 receptor (AT1R) through the tissue renin-angiotensin system plays a pivotal role in the pathogenesis and associated end-organ injury of hypertension. The carboxyl-terminal portion of AT1R is involved in the control of AT1R internalization independent of G protein coupling and plays an important role

\* H. Wakui and K. Tamura contributed equally to this work.

Address for reprint requests and other correspondence: K. Tamura, Dept. of Medical Science and Cardiorenal Medicine, Yokohama City Univ. Graduate School of Medicine, 3-9 Fukuura, Kanazawa-ku, Yokohama 236-0004, Japan (e-mail: tamukou@med.yokohama-cu.ac.jp).

drinking water was administered for the same period. The ANG II and olmesartan dosages were determined from previous reports (10, 18, 48). Following experimental treatment, the mice were anesthetized and the tissues were removed into liquid nitrogen or fixative. The Animal Studies Committee of Yokohama City University approved all the animal experimental protocols.

**Blood pressure measurements.** Systolic blood pressure and heart rate were measured by the tail-cuff method (BP monitor MK-2000; Muromachi Kikai), as described previously (34, 42). BP monitor MK-2000 made it possible to measure blood pressure without pre-heating the animals, thus allowing the avoidance of stressful conditions (17).

**Analysis of total ATRAP and AT1R protein expression.** The characterization and specificity of the anti-mouse ATRAP antibody and the anti-AT1R antibody (sc-1173, Santa Cruz Biotechnology) were described previously (42). Western blot analysis was performed to examine the total protein expression of ATRAP and AT1R as described (40, 42). Briefly, whole tissue extracts were used for SDS-PAGE, and transferred membranes (Millipore) were incubated with either 1) an anti-ATRAP antibody or 2) an anti-AT1R antibody and subjected to enhanced chemiluminescence (Amersham Biosciences). The images were analyzed quantitatively using a Fuji LAS3000 Image Analyzer (Fujifilm) for determination of the total ATRAP and AT1R protein levels. To measure the tissue expression ratio of ATRAP to AT1R, each ATRAP protein level was divided by the corresponding total AT1R protein level obtained by reprobing, and thus was derived from the same extract.

**Real-time quantitative RT-PCR analysis.** Total RNA was extracted from the kidney with ISOGEN (Nippon Gene, Tokyo, Japan), and cDNA was synthesized using the SuperScript III First-Strand System (Invitrogen). Real-time quantitative RT-PCR was performed by incubating the RT product with TaqMan Universal PCR Master Mix and a designed TaqMan probe (Applied Biosystems), essentially as described previously (34). RNA quantity was expressed relative to the 18S rRNA endogenous control.

**Immunohistochemistry for ATRAP and AT1R expression.** Immunohistochemistry was performed as described previously (14, 42). The kidneys were perfusion-fixed with 4% paraformaldehyde, subsequently embedded in paraffin, and cut into sections of 4- $\mu$ m thickness. The sections were dewaxed and rehydrated. Antigen retrieval was performed by microwave heating. The sections were treated for 60 min with 10% normal goat serum in phosphate-buffered saline and blocked for endogenous biotin activity using an Avidin/Biotin Blocking kit (Vector Laboratories). For the study of ATRAP and AT1R, the sections were incubated at 4°C overnight with either 1) an anti-ATRAP antibody diluted at 1:100 or 2) anti-AT1R antibody diluted at 1:100, as described previously (42). The sections were incubated for 60 min with (a) biotinylated goat anti-rabbit IgG (Nichirei), blocked for endogenous peroxidase activity by incubation with 0.3% H<sub>2</sub>O<sub>2</sub> for 20 min, treated for 30 min with streptavidin and biotinylated peroxidase (DAKO), and then exposed to diaminobenzidine. The sections were counterstained with hematoxylin, dehydrated, and mounted. Immunoreactivity was semiquantitatively evaluated in a blinded manner. Briefly, 20 microscopic fields/slide were selected at random for evaluation. Examination was performed using a microscope with  $\times 200$  magnification (Olympus) and an integrated digital camera system (Olympus). Image Pro-plus computer image analysis software (Media Cybernetics, Bethesda, MD) was used to analyze the brown stain pixel density and to quantify the protein levels, as described previously (10, 15, 32, 47).

**Analysis of plasma membrane AT1R expression.** The plasma membrane was specifically extracted from tissues using a Plasma Membrane Extraction Kit (K268-50, Biovision) according to the manufacturer's protocol and then used for SDS-PAGE (43). Membranes (Millipore) were incubated with either 1) anti-AT1R antibody or 2) anti-flotillin-2 monoclonal antibody (no. 3436, Cell Signaling Technology) and subjected to enhanced chemiluminescence (Amer-

sham Biosciences). Flotillin-2 is constitutively localized to the plasma membrane and was used as an internal control protein on the plasma membrane (36). The images were analyzed quantitatively using a Fuji LAS3000 Image Analyzer (Fujifilm) for determination of the plasma membrane AT1R protein levels.

**Generation of ATRAP transgenic mice.** To produce ATRAP transgenic mice, hemagglutinin (HA)-tagged mouse ATRAP cDNA was subcloned into pCAGGS expression vector, which contained a cytomegalovirus enhancer and chicken  $\beta$ -actin (CAG) promoter (28), and the resultant transgene construct was microinjected into the pronuclei of fertilized mouse embryos at the single-cell stage to generate transgenic mice (C57BL/6 strain). The ATRAP transgene positive (+) mice were mated with C57BL/6 wild-type mice to obtain ATRAP transgene positive (+) mice and littermate control mice for the experiments. Animal genotyping was performed as previously described. Transgenic mice were identified by PCR using 5'-TGCTT-

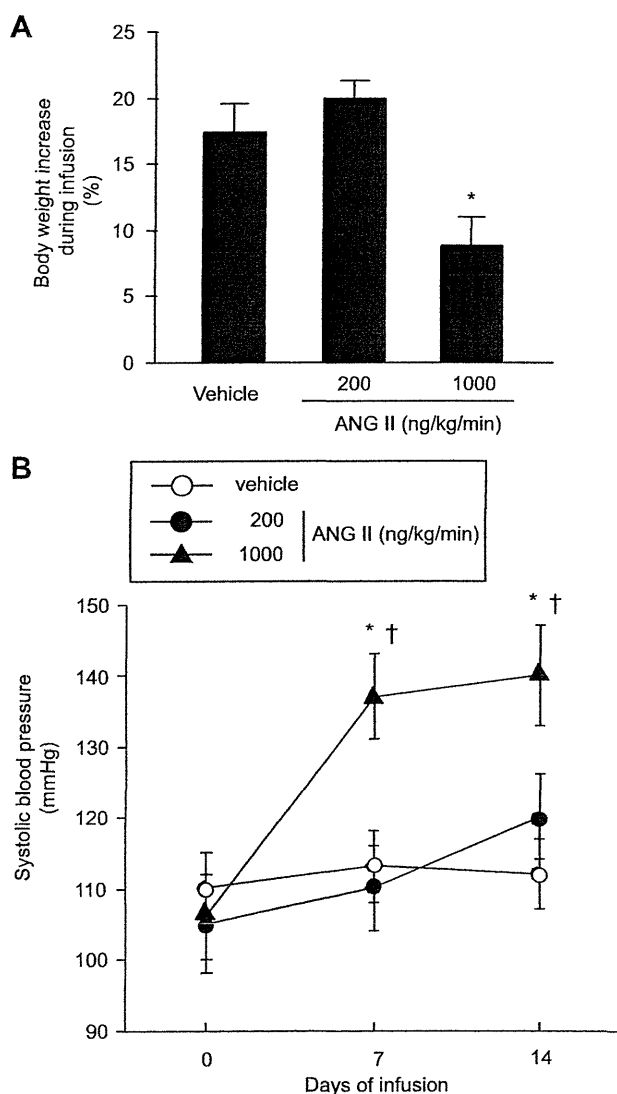


Fig. 1. Effects of continuous ANG II infusion on body weight (A) and systolic blood pressure (B) during the treatment period. Adult male C57BL/6 mice were divided into 3 groups ( $n = 6-8$  mice/group) for the subcutaneous infusion of vehicle or ANG II (either 200 or 1,000  $\text{ng}\cdot\text{kg}^{-1}\cdot\text{min}^{-1}$ ) via an osmotic minipump for 14 days. The values of the percent body weight increase and systolic blood pressure are expressed as means  $\pm$  SE ( $n = 6-8$ /group). \* $P < 0.05$  vs. vehicle. † $P < 0.05$  vs. day 0.

GGGGCAACTTCACTATC-3' as the forward primer and 5'-ACG-GTGCATGTGGTAGACGAG-3' as the reverse primer.

**Statistical analysis.** Values are expressed as means  $\pm$  SE in the text and figures. The data were analyzed using ANOVA. If a statistically significant effect was found, a post hoc analysis with Scheffé's test was performed to detect differences between the groups. Values of  $P < 0.05$  were considered statistically significant.

**RESULTS**

**Effects of ANG II on body weight and systolic blood pressure.** Vehicle-infused mice gained BW during the study period (%BW increase,  $17.2 \pm 2.2\%$ ,  $n = 8$ ) (Fig. 1A). Mice infused at a low dose of ANG II ( $200 \text{ ng}\cdot\text{kg}^{-1}\cdot\text{min}^{-1}$ ) displayed a similar gain in BW (%BW increase,  $19.9 \pm 1.4\%$ ,  $n = 6$ ). In contrast, mice subjected to a high dose of ANG II ( $1,000 \text{ ng}\cdot\text{kg}^{-1}\cdot\text{min}^{-1}$ ) exhibited a significant inhibition of BW gain (%BW increase,  $8.7 \pm 2.1\%$ ,  $n = 7$ ,  $P < 0.05$  vs. vehicle and  $P < 0.01$  vs. ANG II  $200 \text{ ng}\cdot\text{kg}^{-1}\cdot\text{min}^{-1}$ ). All groups displayed the same range of systolic blood pressure, as determined by tail-cuff plethysmography (105–110 mmHg) at base-

line (Fig. 1B). Systolic blood pressure remained stable in the vehicle-infused mice during the study period, with systolic blood pressure averaging  $113 \pm 6$  and  $112 \pm 6$  mmHg by days 7 and 14, respectively ( $n = 8$ ). Similarly, systolic blood pressure did not exhibit any evident change in the low-dose ANG II ( $200 \text{ ng}\cdot\text{kg}^{-1}\cdot\text{min}^{-1}$ )-infused mice ( $110 \pm 5$  and  $120 \pm 5$  mmHg by days 7 and 14, respectively,  $n = 6$ ). In contrast, systolic blood pressure was significantly elevated, to  $137 \pm 6$  and  $140 \pm 7$  mmHg on days 7 and 14 of ANG II infusion, respectively, in the high-dose ANG II ( $1,000 \text{ ng}\cdot\text{kg}^{-1}\cdot\text{min}^{-1}$ )-infused mice. Thus, in this study, the low dose of ANG II ( $200 \text{ ng}\cdot\text{kg}^{-1}\cdot\text{min}^{-1}$ ) corresponds to a subpressor dose, and the high dose of ANG II ( $1,000 \text{ ng}\cdot\text{kg}^{-1}\cdot\text{min}^{-1}$ ) corresponds to a pressor dose.

**Suppression of ATRAP expression by ANG II in the kidney.** We previously showed that ATRAP and AT1R are expressed in various mouse tissues, including the kidney, testis, and liver (42). Thus we examined whether continuous ANG II infusion would regulate ATRAP expression in a tissue-specific manner,

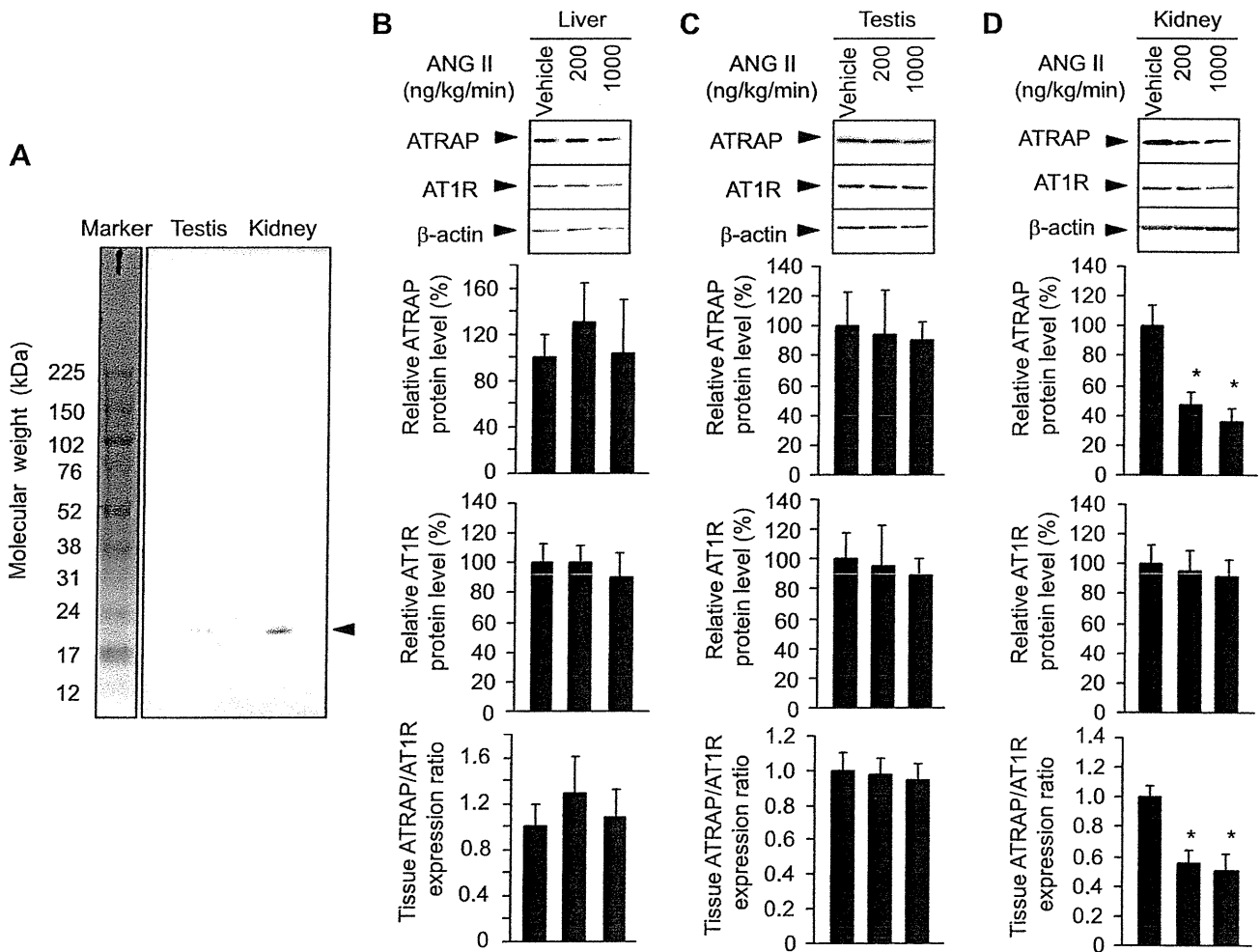


Fig. 2. Western blot showing the signal specificity of the ANG II type 1 receptor (AT1R)-associated protein (ATRAP) protein detected by the polyclonal anti-ATRAP antibody through visualization of the entire size range (A) and representative Western blots showing the effects of continuous ANG II infusion on the total protein expression of ATRAP and AT1R in the tissues of mice infused with vehicle or ANG II ( $200$  or  $1,000 \text{ ng}\cdot\text{kg}^{-1}\cdot\text{min}^{-1}$ ) for 14 days [liver (B); testis (C); kidney (D)]. Measurement of the ATRAP-to-AT1R ratio was performed as described in METHODS. The values were calculated relative to those obtained with extracts from mice infused with vehicle and are expressed as means  $\pm$  SE ( $n = 6/\text{group}$ ). \* $P < 0.05$  vs. vehicle.

using Western blot analysis with an ATRAP-specific antibody (40, 42). Since the antibody developed against ATRAP is relatively new (42), we initially examined the signal specificity through visualization of the entire size range on Western blot analysis. Western blot analysis of tissue extracts from the testis and kidney of adult male C57BL/6 mice revealed that the polyclonal antibody for mouse ATRAP recognized a prominent band of 18 kDa, which was consistent with the predicted molecular mass of mouse ATRAP (= 18 kDa) (Fig. 2A).

Subsequently, we examined whether ANG II stimulation affected the expression of total ATRAP and AT1R expression using whole tissue extracts. The results of Western blot analysis showed that the hepatic and testicular protein levels of both ATRAP and AT1R were similar in the vehicle- and ANG II-infused mice, resulting in no apparent change in the relative expression ratio of ATRAP to AT1R in the liver and testis (Fig. 2, B and C). On the other hand, with respect to the renal expression of ATRAP and AT1R, although the total AT1R protein levels did not exhibit any evident change in either the vehicle-infused or ANG II-infused mice, the ATRAP protein levels at the subpressor and pressor dose in the ANG II-infused mice were significantly lower than in vehicle-infused mice after 14 days of treatment (Fig. 2D). As a result, the relative expression ratio of ATRAP to AT1R in the kidney was significantly suppressed at the subpressor and pressor dose in the ANG II-infused mice compared with the vehicle-infused mice (Fig. 2D; tissue ATRAP/AT1R expression ratio,  $P < 0.05$ , subpressor or pressor dose of ANG II-infused mice vs. vehicle-infused mice).

**Effects of ANG II on mRNA expression of ATRAP, angiotensinogen, NADPH oxidase 4, and  $\alpha$ -subunit of the epithelial sodium channel.** We next examined the pathophysiological consequence of the observed ANG II-induced decreases in renal ATRAP expression by analyzing the mRNA expression of angiotensinogen, NADPH oxidase 4 (Nox4), and the  $\alpha$ -subunit of the epithelial sodium channel ( $\alpha$ -ENaC) in the kidney of

the vehicle- and ANG II-infused mice. For this experiment, we also employed a higher dose of ANG II ( $2,500 \text{ ng} \cdot \text{kg}^{-1} \cdot \text{min}^{-1}$ ) for 2 wk of treatment. Systolic blood pressure was progressively elevated to  $132 \pm 5$  and  $157 \pm 6$  mmHg on *days 7* and *14* of ANG II infusion, respectively, from  $107 \pm 5$  mmHg at baseline, in the higher dose ANG II ( $2,500 \text{ ng} \cdot \text{kg}^{-1} \cdot \text{min}^{-1}$ )-infused mice.

The results of real-time quantitative RT-PCR analysis showed that ANG II infusion (200, 1,000, or  $2,500 \text{ ng} \cdot \text{kg}^{-1} \cdot \text{min}^{-1}$ ) for 14 days led to similarly significant decreases in the renal expression of the ATRAP mRNA compared with vehicle infusion (Fig. 3A). With respect to the renal pathological effects of ANG II stimulation, there were significant elevations of renal angiotensinogen and  $\alpha$ -ENaC mRNA expression by ANG II infusion ( $2,500 \text{ ng} \cdot \text{kg}^{-1} \cdot \text{min}^{-1}$ ), while the renal Nox4 mRNA expression was not affected (Fig. 3, B–D).

**Suppression of ATRAP immunostaining by ANG II in outer medulla of the kidney.** We also examined the effect of ANG II infusion on the intrarenal distribution and expression levels of ATRAP by immunohistochemical analysis. The ATRAP immunohistochemical signal was detected throughout the kidney. A relatively high level of ATRAP immunoreactivity was observed in the outer medulla, and moderate ATRAP immunostaining was also observed in the renal cortex and inner medulla in vehicle-infused mice after 14 days of treatment (Fig. 4). However, there was a significant decrease in ATRAP immunoreactivity in the outer medulla of the kidney in ANG II-infused mice. This suppression of ATRAP expression was likely to be region specific in the outer medulla, since no apparent suppression of ATRAP expression was observed in the inner medulla or cortex (Fig. 4). ANG II infusion did not affect the intrarenal distribution or the relative levels of AT1R immunoreactivity (Fig. 5).

The semiquantitative evaluation with immunohistochemical analysis revealed a region-specific reduction of ATRAP immunostaining in the outer medulla with both the subpressor ( $200 \text{ ng} \cdot \text{kg}^{-1} \cdot \text{min}^{-1}$ ) and pressor ( $1,000 \text{ ng} \cdot \text{kg}^{-1} \cdot \text{min}^{-1}$ )

Fig. 3. Effects of continuous ANG II infusion on ATRAP (A), angiotensinogen (Agt; B), NADPH oxidase 4 (NOX4; C), and the  $\alpha$ -subunit of the epithelial sodium channel ( $\alpha$ -ENaC; D) mRNA expression in the mouse kidney. Real-time quantitative RT-PCR analysis shows the relative ATRAP, Agt, NOX4, and  $\alpha$ -ENaC mRNA levels in the kidney of mice infused with vehicle or ANG II (200, 1,000, or  $2,500 \text{ ng} \cdot \text{kg}^{-1} \cdot \text{min}^{-1}$ ) for 14 days. The values were calculated relative to those obtained with extracts from mice infused with vehicle and are expressed as means  $\pm$  SE ( $n = 6/\text{group}$ ). \* $P < 0.05$  vs. vehicle.

